Oncology and Translational Medicine

Volume 8 • Number 3 • June 2022

Oncology and Translational Medicine Volume 8 • Number 3 • June 2022 pp 109-153

邮发代号：38-121
ISSN 2095-9621

GENERAL INFORMATION
≫otm.tjh.com.cn

ISSN 2095-9621
CN 42-1865/R

Oncology and Translational Medicine

肿瘤学与转化医学（英文）

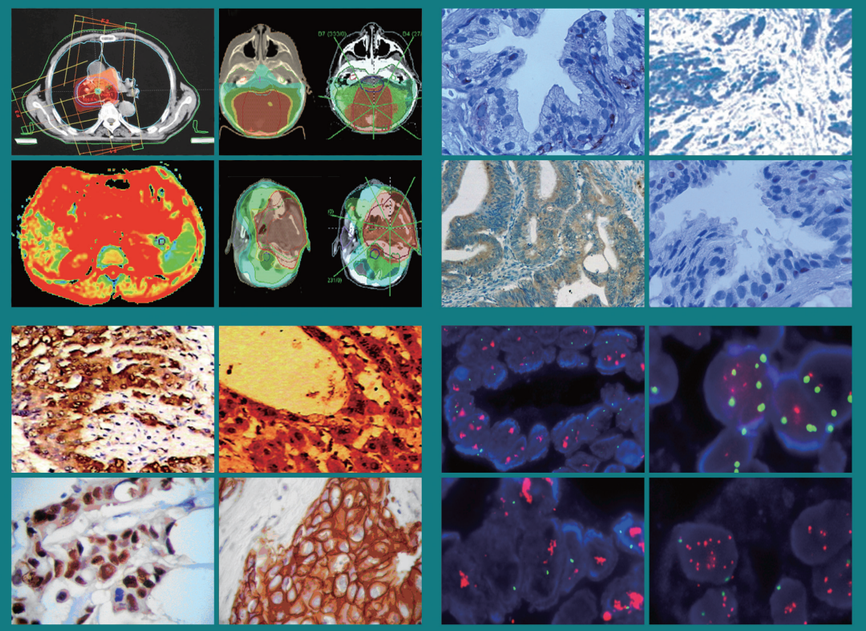

Volume 8
Number 3
June 2022

Oncology and Translational Medicine

Oncology and Translational Medicine
June 2022 Volume 8 Number 3

Contents

Oncology and Translational Medicine

Volume 8 • Number 3 • June 2022

Aims & Scope

Oncology and Translational Medicine is an international professional academic periodical. The Journal is designed to report progress in research and the latest findings in domestic and international oncology and translational medicine, to facilitate international academic exchanges, and to promote research in oncology and translational medicine as well as levels of service in clinical practice. The entire journal is published in English for a domestic and international readership.

Copyright

Supervised by

Ministry of Education of the People's Republic of China.

Administered by

Tongji Medical College, Huazhong University of Science and Technology.

Submission information

Manuscripts should be submitted to:
http://otm.tjh.com.cn
dmedizin@sina.com

Subscription information

ISSN edition: 2095-9621
CN: 42-1865/R

■ Subscription rates
Subscription may begin at any time. Remittances made by check, draft or express money order should be made payable to this journal. The price for 2022 is as follows: US $ 30 per issue; RMB ￥28.00 per issue.

Database

Oncology and Translational Medicine is abstracted and indexed in EMBASE, Index Copernicus, Chinese Science and Technology Paper Citation Database (CSTPCD), Chinese Core Journals Database, Chinese Journal Full-text Database (CJFD), Wanfang Data; Weipu Data; Chinese Academic Journal Comprehensive Evaluation Database.

Business correspondence

All matters relating to orders, subscriptions, back issues, offprints, advertisement booking and general enquiries should be addressed to the editorial office.

Mailing address
Editorial office of
Oncology and Translational Medicine
Tongji Hospital
Tongji Medical College
Huazhong University of Science and Technology
Jie Fang Da Dao 1095
430030 Wuhan, China
Tel.: +86-27-69378388
Email: dmedizin@sina.com

Printer
Changjiang Spatial Information Technology Engineering Co., Ltd. (Wuhan) Hangce Information Cartorgraphy Printing Filial, Wuhan, China
Printed in People's Republic of China

Editors-in-Chief

Managing director

Executive editors

Oncology and Translational Medicine
DOI 10.1007/s10330-021-0547-7

June 2022, Vol. 8, No. 3, P109–P114

ORIGINAL ARTICLE

Prognostic role of plasma levels of γ-glutamyl transpeptidase in patients with advanced gastric cancer treated with anti-PD-1 immunotherapy*

Shaojie Xu[1], Yiming Feng[2] (Co-first author), Xingyin Li[1], Zaozao Huang[3] (✉), Hewei Li[4], Ganxin Wang[5]

[1] First Clinical College, Huazhong University of Science and Technology, Wuhan 430022, China
[2] Department of Radiology, Union Hospital, Tongji Medical College, Huazhong University of Science and Technology, Wuhan 430022, China
[3] Yangchunhu Community Hospital, Liyuan Hospital, Tongji Medical College, Huazhong University of Science and Technology, Wuhan 430077, China
[4] Department of Orthopedics, Liyuan Hospital, Tongji Medical College, Huazhong University of Science and Technology, Wuhan 430077, China
[5] Cancer Center, Union Hospital, Tongji Medical College, Huazhong University of Science and Technology, Wuhan 430022, China

Abstract

Objective Antibodies targeting programmed cell death protein 1 (PD-1) have become the mainstay of treatment for chemotherapy-refractory gastric cancer, characterized by high levels of programmed cell death ligand-1 (PDL-1) expression. However, the routine clinical implementation of PDL-1 testing is currently limited by the lack of robust detection methods. In this regard, the role of plasma γ-glutamyl transpeptidase (GGT), an N-terminal nucleophilic hydrolase, as an independent predictor of the efficacy of anti-PD-1 therapy remains unknown. In this study, we aimed to assessed the prognostic role of changes in plasma GGT levels (6 weeks vs. baseline) in patients with advanced gastric cancer treated with anti-PD-1 immunotherapy.

Methods We retrospectively analyzed data from 57 patients with gastric cancer treated with anti-PD-1 antibodies (camrelizumab, sintilimab, nivolumab, tislelizumab, and toripalimab) at the Union Hospital, Tongji Medical College, Huazhong University of Science and Technology, Wuhan, China, from July 2018 to February 2021.

Results We found that after 6 weeks of treatment, there were significant differences between responders and non-responders with respect to plasma GGT levels ($P < 0.001$). Multivariate logistic regression analysis revealed that the continuous value of the 6-week difference in GGT levels (OR = 1.437, 95% CI = 1.116–1.849, $P = 0.005$) and 6-week difference in GGT ≥ 0 or < 0 (OR = 53.675, 95% CI = 6.379–451.669, $P < 0.001$) were independent predictors of disease control. Survival analysis indicated that a reduction in plasma GGT6 levels during treatment was significantly associated with a favorable progression-free survival (PFS) and overall survival ($P < 0.001$). Consistently, univariate and multivariate Cox regression analyses revealed that a reduction in plasma GGT6 levels during treatment was an independent predictor of PFS (HR = 1.033, 95% CI = 1.013–1.053, $P = 0.001$).

Conclusion Alterations in plasma GGT levels during treatment can be used as a predictor of disease progression and survival in patients with advanced gastric cancer undergoing treatment with anti-PD-1 antibodies.

Key words: gastric cancer; programmed cell death receptor 1; γ-glutamyl transpeptidase (GGT); prognosis

Received: 31 December 2021
Revised: 14 April 2022
Accepted: 21 May 2022

✉ Correspondence to: Zaozao Huang. Email: 2015ly0960@hust.edu.cn
* Supported by a grant from the Hubei and the Huazhong University of Science and Technology Undergraduate Innovation and Entrepreneurship Training Program (No. S202110487427, DYLC2021072).

Targeting immune checkpoints using immune checkpoint inhibitors has become an important treatment method for intractable gastric cancer. In Asian patients with gastric cancer, the anti-programmed cell death protein 1 (PD-1) monoclonal antibody nivolumab has been demonstrated to improve overall survival (OS) rate compared with a placebo treatment [1]. Responses to anti-PD-1 antibodies have been associated with the levels of programmed cell death ligand-1 (PDL-1) expression, with high levels of PDL-1 expression being established to be a predictor of the response to PD1 blockade [2]. Accordingly, plasma high levels of PDL-1 can serve as a prognostic factor predicting good prognosis. However, some patients with PDL-1-positive tumors show early progression in response to anti-PD-1 monotherapy [3]. Furthermore, using PDL-1 expression as a biomarker requires clinical samples and a robust PDL-1 detection method [4], the current lack of which is limiting the utility of PDL-1 as a predictive biomarker. Comparatively, serological biomarkers are readily evaluated and may be useful independent predictors of the response to anti-PD-1 therapy.

Serum γ-glutamyl transpeptidase (GGT) is a cell surface N-terminal nucleophilic hydrolase involved in intracellular oxygen homeostasis. Increased levels of GGT are considered to be indicative of oxidative stress [5], and GGT has also been proposed as a potential prognostic marker for cancer. Indeed, serum levels of GGT have been shown to be associated with the risk of gastric cancer [6], cancer progression, and drug resistance [7]. However, in 65 patients with gastric cancer, Wang *et al* [8] found serum GGT to be a poor prognostic factor for this disease. Nonetheless, the predictive value of GGT levels in patients receiving anti-PD-1 therapy remains to be determined. In this study, we investigated the utility of plasma GGT levels with respect to predicting the response to anti-PD-1 therapy in patients with gastric cancer.

Patients and methods

Patients

For the purposes of this study, we assessed the data obtained for 57 patients (34 men and 23 women) with gastric cancer who had undergone treatment with anti-PD-1 antibodies (camrelizumab, sintilimab, nivolumab, tislelizumab, and toripalimab) at the Union Hospital, Tongji Medical College, Huazhong University of Science and Technology, Wuhan, China, from July 2018 to February 2021. Inclusion criteria for patient enrolment were as follows: (1) diagnosis of primary gastric cancer after pathological biopsy, (2) metastatic gastric cancer treated with at least two cycles of PD-1 blockade, and (3) complete clinicopathological and follow-up data. The exclusion criteria were as follows: (1) diagnosis of other tumors or recurrent gastric cancer, (2) liver or kidney dysfunction, and (3) tumor HER2 negativity determined by genetic testing. The study was approved by the Hospital Ethics Review Committee. All study procedures complied with the ethical standards of the Ethics Review Committee and the ethical requirements of the Declaration of Helsinki. To obtain the consent of patients, we adopted an opt-out approach in this retrospective study.

Data collection

We collected patients' baseline characteristics and clinical data, including age, gender, treatment with radiotherapy or chemotherapy, metastatic status (distant organ metastasis, peritoneal metastasis, distant organ and peritoneal metastasis), lines of therapy (first-line, second-line, or third-line and above), and GGT levels. Clinical response was determined according to the Response Evaluation Criteria in Solid Tumors (RECIST) as a complete response (CR), partial response (PR), stable disease (SD), or progressive disease (PD). CR, PR, and SD were considered as a response, and PD was considered non-response. Plasma GGT levels were evaluated on the first day of anti-PD-1 treatment (baseline) and after 6 weeks of treatment. The difference between these two points was also calculated.

Data analysis

Data are expressed as the median (range), mean ± standard deviation, or numerical (percentage) values. Continuous variables were compared using a *t*-test, and categorical variables were analyzed using Pearson's chi-squared test or Fisher's exact test. Numerical variables that did not meet the conditions of normality and homogeneity of variance were analyzed using a rank-sum test. Univariate and multivariate Cox logistic regression analyses were conducted to identify risk factors associated with disease progression. Two-sided P-values ≤ 0.05 were considered to indicate statistical significance. Survival analysis was performed using the Kaplan-Meier method and the log-rank test. SPSS 26.0 software (Statistical Package for the Social Sciences, IBM Corp., Armonk, NY, USA) was used for all statistical analyses.

Results

Patient characteristics and tumor response

The baseline characteristics of the 57 patients included in this study are summarized in Table 1. The median age of the patients was 56 years (range, 23–76). Among the 57 patients, 34 (59.6%) were men. Twenty-eight (49.1%) patients received surgery, 49 (85.9%) received chemotherapy, 19 (33.3%) received first-line PD-1 blockade, 20 (35.1%) received second-line PD-1 blockade,

Table 1 Patient characteristics [*n* (%)]

Variable	*n* = 57
Age: Median (range, years)	56 (23–76)
Sex: Male/female	34/23
Metastasis: Organ/peritoneum/organ and peritoneum	31/9/17
Surgery: Yes/no	28/29
Chemotherapy: Yes/no	49/8
Lines of anti-PD-1 therapy: 1/2/≥ 3	19/20/18
Objective tumor response	
Complete response	0 (0%)
Partial response	10 (14.0%)
Stable disease	13 (17.5%)
Progressive disease	34 (59.6%)

and 18 (31.6%) received third-line PD-1 blockade or above. None of the patients had CR, eight (14.0%) had PR, 10 (17.5%) had SD, and 34 (59.6%) had PD.

Differences in clinicopathological characteristics between responders and non-responders

Differences in the clinicopathological characteristics of responders and non-responders are shown in Table 2. Responders were found to be characterized by a reduction in GGT levels from baseline, whereas non-responders showed an increase in GGT levels during treatment, and the difference in the change in GGT levels between responders and non-responders was found to be statistically significant ($P < 0.001$).

Factors predicting the response to PD-1 blockade

To identify factors predicting a treatment response, we performed univariate and multivariate logistic regression analyses (Table 3). Univariate analysis revealed the following to be significant predictors of the response to PD-1 blockade: peritoneal metastasis [odds ratio (OR) = 0.201, 95% confidence interval (CI) = 0.048–0.841, P = 0.028], continuous 6-week difference in GGT (change in GGT levels from baseline, as a continuous variable) (OR = 1.365, 95% CI = 1.122–1.661, P = 0.002), and 6-week difference in GGT < 0 (patients with reduced GGT levels during treatment) (OR = 23.619, 95% CI = 5.371–103.858, $P < 0.001$). Multivariate regression analysis revealed that the continuous value of the 6-week difference in GGT (OR = 1.437, 95% CI = 1.116–1.849, P = 0.005) and the 6-week difference in GGT ≥ 0 or < 0 (OR = 53.675, 95% CI = 6.379–451.669, $P < 0.001$) were independent factors predicting the response to anti-PD-1 treatment.

Table 3 Factors predicting the response to PD-1 blockad

Variable	Odds ratio	95% CI	*P*-value
Univariate analysis			
Age	0.992	0.948–1.038	0.726
Sex: Male	1.089	0.370–3.208	0.877
Metastasis			
Peritoneum	0.201	0.048–0.841	0.028*
Distant organs and peritoneum	0.268	0.044–1.640	0.154
Surgery: Yes	0.917	0.318–2.643	0.872
Chemotherapy: Yes	1.149	0.246–5.365	0.859
Lines of therapy			
2	0.364	0.095–1.386	0.138
≥ 3	1.167	0.297–4.588	0.825
GGT			
Baseline	1.002	0.995–1.008	0.640
6 weeks	1.010	0.993–1.027	0.255
6-week difference (continuous)	1.365	1.122–1.661	0.002*
6-week difference (< 0)	23.619	5.371–103.858	0.000*
Multivariate analysis: GGT			
6-week difference (continuous)	1.437	1.116–1.849	0.005*
6-week difference (< 0)	53.675	6.379–451.669	0.000*

Note: * $P < 0.05$

Survival analysis

Kaplan-Meier analysis revealed that progression-free survival (PFS) was significantly higher in patients with increased GGT levels during treatment than in those with reduced GGT levels during treatment ($P < 0.001$; Fig. 1). The mean PFS time of patients in the GGT group with a 6-week difference < 0 and a 6-week difference ≥ 0 was

Table 2 Differences in clinicopathological characteristics between responders and non-responders (*n*)

Variable	Responders (*n* = 23)	Non-responders (*n* = 34)	*P*-value
Age: Mean (years, SD)	55.52 (10.58)	54.41 (12.75)	0.732 [a]
Sex: Male/female	14/9	20/14	1.000 [b]
Metastasis: Organ/peritoneum/both	16/4/3	15/5/4	0.079 [c]
Surgery: Yes/no	11/12	17/17	1.000
Chemotherapy: Yes/no	3/20	5/29	0.590 [c]
Lines of therapy: 1/2/≥ 3	11/6/6	8/14/12	0.158 [b]
GGT (median, IQR)			
Baseline	28.00 (17.00, 36.00)	21.50 (14.00, 47.50)	0.425 [d]
6 weeks	24.00 (17.00, 34.00)	28.50 (17.75, 72.50)	0.286 [d]
6-week difference	–2 (–6.00, 0.00)	5.50 (2.00, 20.00)	< 0.001*

Note: * $P < 0.05$; [a] *t*-test; [b] Chi-square test; [c] Fisher exact test; [d] Rank-sum test

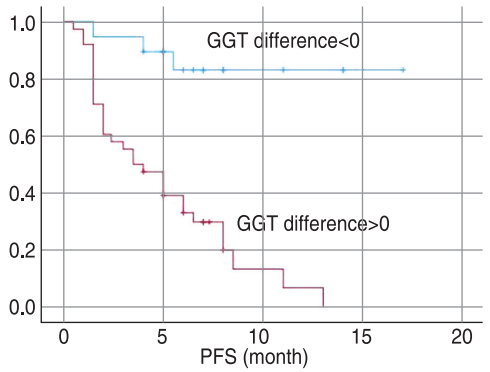

Fig. 1 Kaplan-Meier survival curves for progression-free survival stratified by γ-glutamyl transpeptidase (GGT)

14.765 and 4.954 months, respectively.

Univariate and multivariate Cox regression analysis of progression-free survival

Cox regression analysis was performed to assess the relationship between alterations in GGT levels during treatment and PFS (Table 4). Univariate (HR = 8.916, 95% CI = 2.693–29.516, $P < 0.001$) and multivariate (HR = 1.033, 95% CI = 1.013–1.053, $P = 0.001$) regression analysis revealed a 6-week difference in GGT < 0 to be an independent predictor of PFS.

Table 4 Univariate and multivariate Cox analyses of progression-free survival

Variable	Hazard ratio	95% CI	*P*-value
Univariate analysis			
Age	0.990	0.960–1.021	0.514
Sex	0.924	0.465–1.835	0.882
Metastasis			
Peritoneum	0.448	0.214–0.938	0.033
Distant organs and peritoneum	0.639	0.228–1.794	0.395
Surgery	0.839	0.427–1.649	0.611
Chemotherapy	0.978	0.377–2.536	0.963
Lines of therapy			
2	0.553	0.222–1.376	0.203
≥ 3	1.301	0.593–2.857	0.511
GGT baseline	1.001	0.999–1.004	0.325
GGT 6-week difference (< 0)	8.916	2.693–29.516	0.000*
Multivariate analysis			
GGT 6-week difference (< 0)	1.033	1.013–1.053	0.001*

Note: *$P < 0.05$

Discussion

Gastric cancer is among the major causes of cancer-related death worldwide. Although patients with early-stage gastric cancer can be treated with surgery, mortality rates remain high. Given the lack of effective screening strategies, most Chinese patients with gastric cancer are diagnosed at an advanced stage of disease progression [9]; thus, treatment options for these patients remain limited, and the prognosis is relatively poor. The key roles of immune checkpoints, including PD-1 and PDL-1, as immune escape mechanisms have been extensively demonstrated, and anti-PD-1/PD-L1 antibodies are used to treat a number of cancers, notably renal and lung cancers [10]. PD-1 blockade has also been shown to have a good safety profile and high efficacy in patients with gastric cancer [1]. Nevertheless, despite the promising prognostic value of PDL-1 levels in gastric cancer, its clinical application remains limited. As an alternative, in this study, we evaluated the prognostic utility of GGT levels in patients with advanced gastric cancer treated with PD-1 blockade. We found that alterations in GGT levels during treatment could be used to predict the response to anti-PD-1 therapy. Notably, an increase in GGT levels during treatment was found to be associated with disease progression and poor survival in patients undergoing anti-PD-1 therapy. To the best of our knowledge, this is the first study to demonstrate the prognostic role of GGT levels during treatment in patients with advanced gastric cancer treated with anti-PD-1 antibodies.

In humans, plasma GGT is predominantly derived from the liver and is accordingly used as an indicator of liver dysfunction and obstructive liver disease. Given that sex, diet, liver dysfunction, and kidney dysfunction are key factors affecting plasmas levels of GGT, patients with hepatic and renal dysfunction were excluded from this study. Interestingly, we found that metastasis in distant organs, including the liver, is unassociated with a response to anti-PD-1 therapy in patients with gastric cancer. The findings of a previous meta-analysis have indicated that baseline GGT levels are correlated with the overall cancer risk (RR = 1.32, 95% CI = 1.15–1.52), as well as with the risk of digestive cancer (RR = 1.94, 95% CI = 1.35–2.79) [11]. In addition, high GGT levels have been found to be associated with a poor prognosis in patients with liver, breast, renal cell, and endometrial cancers [12]. However, the role of GGT in carcinogenesis is yet to be sufficiently clarified. Corti *et al* [13] found that high GGT levels can lead to enhanced iron intake, the generation of hydroxyl radicals, and DNA damage. In turn, genomic instability and gene mutations can suppress immune responses and promote the proliferation of cancer cells, thereby leading to disease progression [14]. Moreover, GGT has been observed to promote the hydrolysis and peptide transfer of extracellular glutathione, glutathione degradation, oxidative stress, and reactive oxygen species generation, thereby further enhancing cancer cell proliferation and drug resistance [15–16]. To some extent, these mechanisms can provide an explanation to account for the poor prognosis of patients with gastric cancer and increased

GGT levels during anti-PD-1 treatment.

It has previously been shown that GGT levels are significantly correlated with OS in patients with advanced gastric cancer (HR = 1.006, 95% CI = 1.003–1.009, $P < 0.001$) [17]. To assess the relationship between the dynamic changes in GGT levels and prognosis in patients treated with anti-PD-1 antibodies, we conducted survival and multivariate Cox regression analyses. We accordingly established that an increase in GGT levels during treatment was associated with a favorable prognosis and improved survival. Importantly, multivariate Cox regression analysis identified an increase in GGT levels during treatment as an independent predictor of PFS, thereby indicating that alterations in the levels of GGT during PD-1 blockade can be used to predict treatment response and prognosis in patients with advanced gastric cancer.

In the cohort assessed in this study, we detected no significant difference between the baseline and 6-week values of GGT among responders and non-responders. Contrastingly, alterations in GGT levels during treatment were found to differ significantly between these two groups ($P < 0.001$). In the responders, we noted a reduction in GGT levels during treatment, whereas in the non-responders, there were increases in the levels of GGT during immunotherapy. Consistently, the findings of multivariate logistic regression analysis indicated that a reduction in GGT levels during treatment can serve as an independent predictor of disease control. These findings accordingly indicate that the direction of alterations in GGT levels during treatment can be used to predict the response to PD-1 blockade in patients with advanced gastric cancer.

In addition to plasma GGT levels, we also identified peritoneal metastasis as being associated with a treatment response in patients with gastric cancer, which is consistent with findings of previous clinical studies in which patients with gastric cancer received systemic chemotherapy [18]. These findings would thus tend to indicate that metastatic tumor cells in the peritoneum may act as a barrier that prevents drugs from reaching their therapeutic targets.

Despite our promising findings, this study does have an important limitation, in that it was a single-center retrospective study with a small cohort size. Consequently, our results need to be further confirmed by large-scale multi-center prospective trials. In addition, there was a lack of uniformity in the lines of treatment among patients, and thus whether GGT is a prognostic factor of anti-PD-1 antibody anti-tumor effect in patients receiving the same therapeutic line again needs to be further confirmed. Moreover, the efficacy of other clinicopathological variables in predicting an anti-PD-1 treatment response merits further investigation.

In conclusion, our findings provide convincing evidence that alterations in plasma GGT levels during anti-PD-1 therapy independently predict disease progression and poor survival in patients with advanced gastric cancer. These findings also indicate that plasma GGT levels can be used as a marker to predict the response to anti-PD-1 immunotherapy in these patients.

Acknowledgments

Not applicable.

Funding

This study was supported by the Hubei and the Huazhong University of Science and Technology Undergraduate Innovation and Entrepreneurship Training Program (No. S202110487427, DYLC2021072).

Conflicts of interest

All authors have completed the ICMJE uniform disclosure form. The authors have no conflicts of interest to declare.

Author contributions

All authors contributed to data acquisition, data interpretation, and reviewed and approved the final version of this manuscript.

Data availability statement

All data generated or analyzed during this study are included in this published article (and the accompanying supplementary information files).

Ethical approval

Not applicable.

References

1. Kang YK, Boku N, Satoh T, et al. Nivolumab in patients with advanced gastric or gastro-oesophageal junction cancer refractory to, or intolerant of, at least two previous chemotherapy regimens (ONO-4538-12, ATTRACTION-2): a randomised, double-blind, placebo-controlled, phase 3 trial. Lancet. 2017;390(10111):2461-2471.
2. Fuchs CS, Doi T, Jang RW, et al. Safety and efficacy of pembrolizumab monotherapy in patients with previously treated advanced gastric and gastroesophageal junction cancer: Phase 2 clinical KEYNOTE-059 trial. JAMA Oncol. 2018;4(5):e180013.
3. Tabernero J, Van Cutsem E, Bang Y, et al. Pembrolizumab with or without chemotherapy versus chemotherapy for advanced gastric or gastroesophageal junction (G/GEJ) adenocarcinoma: The phase III KEYNOTE-062 study. JCO.2019;37(18_suppl):A4007.
4. Guo XJ, Cao H, Zhou JY, et al. Progress on the study of PD-L1 detection methods in non-small cell lung cancer. Chin J Lung Cancer (Chinese).2019;22(1):40-44.
5. Terzyan SS, Burgett AW, Heroux A, et al. Human γ-Glutamyl transpeptidase 1: structures of the free enzyme, inhibitor-bound tetrahedral transition states, and glutamate-bound enzyme reveal

novel movement within the active site during catalysis. J Biol Chem. 2015;290(28):17576-17586.
6. Mok Y, Son DK, Yun YD, et al. γ-Glutamyltransferase and cancer risk: The Korean cancer prevention study. Int J Cancer. 2016;138(2):311-319.
7. Corti A, Franzini M, Paolicchi A, et al. Gamma-glutamyltransferase of cancer cells at the crossroads of tumor progression, drug resistance and drug targeting. Anticancer Res. 2010;30(4):1169-1181.
8. Wang Q, Shu X, Dong Y, et al. Tumor and serum gamma-glutamyl transpeptidase, new prognostic and molecular interpretation of an old biomarker in gastric cancer. Oncotarget. 2017;8(22):36171-36184.
9. Ma X, Wang Y, Fan H, et al. Genetic polymorphisms of Cathepsin B are associated with gastric cancer risk and prognosis in a Chinese population. Cancer Biomark. 2021;32(2):189-198.
10. Han EQ, Li XL, Wang CR, et al. Chimeric antigen receptor-engineered T cells for cancer immunotherapy: progress and challenges. J Hematol Oncol. 2013;6:47.
11. Kunutsor SK, Apekey TA, Van Hemelrijck M, et al. Gamma glutamyltransferase, alanine aminotransferase and risk of cancer: systematic review and meta-analysis. Int J Cancer. 2015;136(5):1162-1170.
12. Sun L, Yin W, Wu Z, et al. The predictive value of pre-therapeutic serum gamma-glutamyl transferase in efficacy and adverse reactions to neoadjuvant chemotherapy among breast cancer patients. J Breast Cancer. 2020;23(5):509-520.
13. Corti A, Duarte TL, Giommarelli C, et al. Membrane gamma-glutamyl transferase activity promotes iron-dependent oxidative DNA damage in melanoma cells. Mutat Res. 2009;669(1-2):112-121.
14. Salnikow K. Role of iron in cancer. Semin Cancer Biol. 2021;76:189-194.
15. Cordani M, Butera G, Pacchiana R, et al. Mutant p53-associated molecular mechanisms of ROS regulation in cancer cells. Biomolecules. 2020;10(3):361.
16. Stark AA, Russell JJ, Langenbach R, et al. Localization of oxidative damage by a glutathione-gamma-glutamyl transpeptidase system in preneoplastic lesions in sections of livers from carcinogen-treated rats. Carcinogenesis. 1994;15(2):343-348.
17. Yang S, He X, Liu Y, et al. Prognostic significance of serum uric acid and gamma-glutamyltransferase in patients with advanced gastric cancer. Dis Markers. 2019;2019:1415421.
18. He YL. Surgical treatment for peritoneal metastasis from gastric cancer. Chin J Oncol (Chinese). 2019;41(3):173-177.

DOI 10.1007/s10330-021-0547-7
Cite this article as: Xu SJ, Feng YM, Li XY, et al. Prognostic role of plasma levels of γ-glutamyl transpeptidase in patients with advanced gastric cancer treated with anti-PD-1 immunotherapy. Oncol Transl Med. 2022;8(3):109–114.

Oncology and Translational Medicine
DOI 10.1007/s10330-021-0526-6

June 2022, Vol. 8, No. 3, P115–P120

ORIGINAL ARTICLE

Occurrence of No.12 lymph node micrometastasis in gastric cancer and its effect on clinicopathological parameters and prognosis*

Tianzeng Dong[1] (✉), Lirong Zhang[2]

[1] Emergency Department, Handan People's Hospital, Handan 056001, China
[2] Department of Neurology, General Hospital of Jizhong Energy Fengfeng Group Co. LTD., Handan 056200, China

Abstract

Objective This study aimed to investigate the occurrence of No.12 lymph node micrometastasis in patients with gastric cancer and its relationship with clinicopathological parameters and prognosis.

Methods A cohort of 160 gastric cancer patients who underwent gastrectomy and lymph node dissection were selected as the research subjects. The immunohistochemical method was used to detect the micrometastasis of No.12 lymph node sections with negative routine pathological detection. At the same time, the clinical data of patients were collected and followed up to analyze the clinical significance of No.12 lymph node micrometastasis.

Results A total of 370 No.12 lymph nodes were detected in 160 surgical specimens. Among 160 patients, 27 patients were found to be positive for No.12 lymph nodes during routine pathological examination, with a positive rate of 16.8%. A total of 308 lymph nodes from 133 patients with negative routine pathological examinations were stained by immunohistochemistry. A total of 17 lymph nodes from 10 patients were found to be positive. The results showed that 37 of the 160 patients had No.12 lymph node metastasis, and the positive rate was 23.1%, which was 6.3% higher than that of routine pathological examination. Logistic multivariate analyses showed that the depth of invasion, lymph node metastasis in other groups, and clinical stage were independent risk factors for No.12 lymph node metastasis. The average follow-up time was 79.3 months, and the overall median survival time was 47.9 months. The survival time of the No.12 lymph node-negative group was 67.3 ± 2.5 Â months, the median survival time was 73.2 months; the survival time of the No.12 lymph node-positive group was (28.4 ± 5.4) months, and the median survival time was 31.3 months. The survival time of the No.12 lymph node-negative group was significantly longer than that of the positive group (χ^2 = 12.75, P = 0.000).

Conclusion No.12 lymph node micrometastasis is a signal affecting the prognosis of patients with gastric cancer. Standardized dissection of No.12 lymph nodes is recommended for patients with gastric cancer who can undergo radical resection.

Received: 28 September 2021
Revised: 11 November 2021
Accepted: 21 January 2022

Key words: gastric tumor; lymphatic metastasis; micrometastasis

Gastric cancer is one of the most common gastrointestinal malignancies. Compared with Japan, South Korea, and other countries, the detection rate of early gastric cancer in China is low. Many patients are first diagnosed with gastric cancer when they have already progressed to the advanced stage and already lost the best treatment opportunity [1]. At present, the scientific nature of radical surgery based on D2 lymph node dissection is widely recognized, but there are still some debates on the scope and strategy of some local dissection [2]. The hepatoduodenal ligament is an important anatomical marker in radical gastrectomy for gastric cancer. It has important structures, such as the biliary tract, portal vein, and proper artery. It is prone to complications such as lymphatic leakage and bile leakage after surgery. Therefore, cleaning the tissue

✉ Correspondence to: Tianzeng Dong. Email: dongtianzeng23@163.com
* Supported by a grant from the Hebei Medical Science Research Project (No. 20191831).

in this area has high technical requirements for the operator [3]. Regional lymph node metastasis is the main factor affecting the prognosis of patients with gastric cancer. Accurate determination of lymph node status is of great significance for the rational selection of surgical methods and accurate judgment of patient prognosis [4]. Lymph node micrometastasis (LNM) is a special form of metastasis and its clinical significance in patients with gastric cancer remains controversial [5]. In this study, 160 patients with gastric cancer who underwent D2 or above radical surgery were studied to explore the occurrence law of No.12 lymph node micrometastasis and its impact on clinicopathological parameters and prognosis.

Materials and methods

Research object

From January 2012 to January 2016, we collected the clinical data of gastric cancer patients in the General Hospital of Jizhong Energy Fengfeng Group Co., Ltd. The inclusion criteria were: (1) Radical lymphadenectomy with D2 or above; (2) None of the patients received radiotherapy or neoadjuvant chemotherapy before surgery; (3) All patients were diagnosed with gastric cancer for the first time; (4) Their ages ranged from 30 to 70 years. Exclusion criteria: (1) Patients with residual gastric cancer; (2) Combined with other malignant tumors or a history of malignant tumors; or (3) The clinical and follow-up data were incomplete. Finally, 160 patients were included in the study, including 154 patients with advanced gastric cancer (96.2%) and 6 patients with early gastric cancer (3.8%) comprising 88 males and 72 females. There were 99 elderly patients aged above 60 years. The tumor was mainly located in the lower 1/3, with a total of 94 cases. The tumors were located in the upper 1/3, middle 1/3, trans regional, or whole stomach in 32 cases, 27 cases, and 7 cases, respectively. According to the Borrmann classification, there were 9 cases of type I, 43 cases of type II, 90 cases of type III, and 18 cases of type IV. The clinical stages were generally delayed. There were 36 cases of stage I + II and 124 cases of stage III and IV. Serum carcinoembryonic antigen (CEA) level was normal in 142 cases, increased in 18 cases; serum CA19-9 level was normal in 145 cases, and increased in 15 cases.

No.12 lymph node dissection steps

The omentum was cut close to the lower edge of the liver, the visceral peritoneum of the hepatoduodenal ligament was cut horizontally, and the proper hepatic artery, the front of the common bile duct, and the right gastric artery were dissected individually. The duodenal peritoneum was opened by Kocher incision to reach the rear of the duodenum, the right peritoneum of the hepatoduodenal ligament was cut, the right edge of the common bile duct was exposed, and the No.12b and No.12a lymph nodes were cleaned. The posterior wall was then stripped from the back of the portal vein, the cleaned tissue was pulled to the upper left, the No.12p lymph nodes around the portal vein were cleaned, and then stripped to the bifurcation of the common hepatic artery and gastroduodenal artery. So far, the No.12 lymph node has been cleaned.

Detection of clinical metastasis and micrometastasis of lymph nodes

According to the operation specifications of the kit, No.12 lymph node sections with negative routine pathological examination were detected for micrometastasis by immunohistochemical analysis. Cytokeratin CK20 was detected using a two-step method. The main operation steps include slicing, dewaxing, antigen repair, elimination of endogenous peroxidase activity by hydrogen peroxide, dropping primary antibody (mouse anti-human CK20 monoclonal antibody, Bode company), secondary antibody incubation, DAB color development, counterstaining, dehydration, transparency, sealing, and microscopic examination.

Follow up

Follow-up was mainly conducted through telephone and outpatient visits. The duration of follow-up was once every 3 months in the first year, once every half a year in the second year, and once every year in the third year and after. The follow-up period was until January 2021. According to the condition of the patients, routine blood examination, biochemical examination, or thoracoabdominal basin CT and endoscopy were performed. Nutritional deficiencies, such as those of vitamin B12 and iron were closely monitored and treated, if necessary.

Statistical analyses

All data were statistically analyzed using SPSS software (version 20.0). The relationship between No.12 lymph node metastasis and clinicopathological parameters was analyzed using the chi square test, Fisher's exact probability method, and multivariate analyses was performed using the logistic risk model. The log-rank test was used to compare the effect of No.12 lymph node metastasis on the prognosis of patients with gastric cancer. Inspection level $\alpha = 0.05$. Statistical significance was set at $P < 0.05$.

Results

Routine pathological examination and immunohistochemical staining were used to detect lymph node metastasis and

micrometastasis

A total of 370 No.12 lymph nodes were detected in 160 surgical specimens. Among the 160 patients, 27 patients were positive for No.12 lymph nodes during routine pathological examination, with a positive rate of 16.8%. A total of 308 lymph nodes from 133 patients with negative routine pathological examinations were stained by immunohistochemistry. A total of 17 lymph nodes from 10 patients were found to be positive. The results showed that 37 of the 160 patients had No.12 lymph node metastasis, and the positive rate was 23.1%, which was 6.3% higher than that of routine pathological examination (Fig. 1).

Univariate analysis of the effects of No.12 lymph node metastasis and micrometastasis on clinicopathological parameters

Univariate analysis showed that the occurrence of No.12 lymph node clinical metastasis was related to Borrmann classification, lymph node metastasis, and clinical stage of gastric cancer ($P < 0.05$). The results showed that the occurrence of No.12 lymph node micrometastasis was only related to the Borrmann classification, lymph node metastasis, and clinical stage of gastric cancer ($P < 0.05$) (Table 1).

Multivariate analyses of the influence of No.12 lymph node metastasis on clinicopathological parameters

The pathological factors, including tumor location, No.12 lymph node metastasis, lymph node metastasis in other groups, clinical stage, degree of differentiation, and tumor diameter were included in the logistic risk model for multivariate analyses. The results showed that the depth of invasion, lymph node metastasis in other groups, and clinical stage were independent risk factors affecting No.12 lymph node metastasis (Table 2).

Follow up results

The average follow-up time was 79.3 months, and the overall median survival time was 47.9 months. The survival time of the No.12 lymph node-negative group was 67.3 ± 2.5 Â months, the median survival time was 73.2 months; the survival time of the No.12 lymph node-positive group was 28.4 ± 5.4) months, and the median survival time was 31.3 months; and the difference between the two groups was statistically significant ($\chi^2 = 12.75$, $P = 0.000$).The survival time of the No.12 lymph node-negative group was significantly longer than that of the positive group (Fig. 2).

Discussion

In 1971, Huvos discovered the phenomenon of lymph node micrometastases in breast cancer for the first time. It was defined as a non-metastatic tumor with a diameter less than 2 mm, which is difficult to detect by routine pathological examination. In 1998, the international alliance against cancer (UICC) updated this concept and defined a single tumor cell or cell cluster with a diameter of < 0.2 mm as “isolated tumor cell nest” (ITC). This concept is still used today. Therefore, the most accurate definition of LNM is the tumor cell cluster with 0.2 mm ≤ r < 2 mm [6].

In China, D2 lymph node dissection is generally recognized as the standard surgical method for patients with gastric cancer. The Japanese Gastric Cancer Association divides the lymph nodes into three stations and 16 groups of lymph nodes according to the gastric omentum and large blood vessels around the stomach [7]. Groups 1 to 6 belong to the first stop, including the left and right of the cardia, large and small curvatures of the stomach, and upper and lower pylorus. The second and third stations, that is, groups 7–16, include the total liver, pancreas, posterior duodenum, celiac trunk, left stomach, splenic artery and hilar lymph nodes, superior mesenteric artery lymph nodes, and para-aortic lymph nodes [8].

The hepatoduodenal lymph nodes are no.12a along the hepatic artery, no.12b along the bile duct, and no.12p behind the portal vein [9]. There are many methods for detecting LNM. The serial section method was first used in the clinic, but it is difficult to detect a small number of cancer cells because of its heavy workload. RT-PCR has high specificity and sensitivity, but it has high requirements for experimental technology, is uneconomical, and has not been fully popularized. Therefore, at present, the most commonly used method for detecting LNM is the immunohistochemical method, which is economical, easy to perform, and widely used [10].

A total of 370 No.12 lymph nodes were detected in 160 surgical specimens. Among the 160 patients, 27 patients were positive for No.12 lymph nodes during routine pathological examination, with a positive rate of 16.8%. Furthermore, cytokeratin CK20, with high sensitivity, was used to detect micrometastases. A total of 308 lymph nodes from 133 patients with negative routine pathological examinations were stained by immunohistochemistry. A total of 17 lymph nodes in 10 patients were found to be positive. The results showed that 37 of the 160 patients had No.12 lymph node metastasis, and the positive rate was 23.1%, which was 6.3% higher than that of routine pathological examination. As an important defense line of human immune function, the lymphatic system will be significantly damaged by the expansion of intraoperative

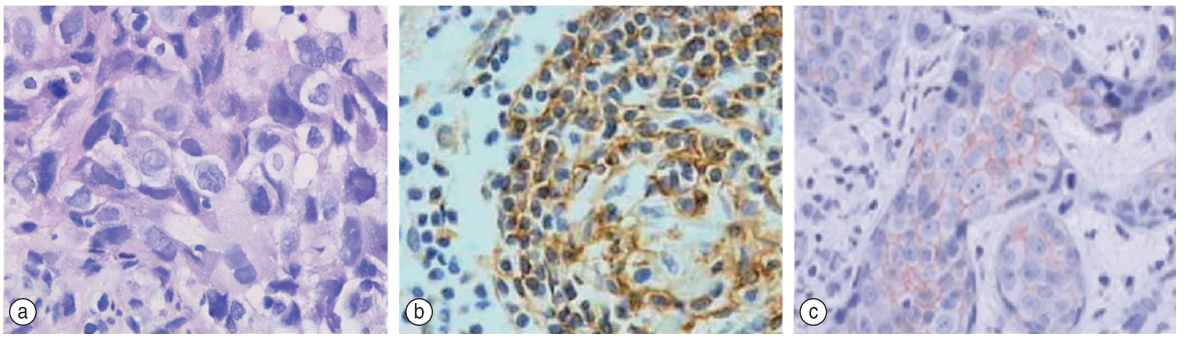

Fig. 1 Routine pathological examination and immunohistochemical staining of the lymph nodes

Table 1 Comparison of the effects of No.12 lymph node metastasis and micrometastasis on each clinicopathological parameter

Index	No.12 Conventional pathology (+)	No.12 Conventional pathology (–)	χ^2	*P*	No.12 (+)	No.12 (–)	χ^2	*P*
Gender			0.004	0.949			0.784	0.376
Female	15	73			18	70		
Male	12	60			19	53		
Age (years)			0.316	0.574			0.182	0.669
< 60	9	52			13	48		
≥ 60	18	81			24	75		
Tumor site			3.543	0.315			6.319	0.097
Upper 1/3	5	27			6	26		
Middle 1/3	4	23			5	22		
Down 1/3	15	79			17	77		
Whole stomach	3	4			4	3		
Differentiation			0.157	0.692			0.041	0.839
Low	17	89			24	82		
Middle-high	10	44			13	41		
Borrmann			15.944	0.001			41.581	0.000
I	1	8			1	8		
II	6	37			6	37		
III	11	79			15	75		
IV	9	9			15	3		
Lauren			0.077	0.781			2.664	0.103
intestinal	15	70			24	61		
diffuse	12	63			13	62		
Size (cm)			0.054	0.816			0.065	0.799
< 5	16	82			22	76		
≥ 5	11	51			15	47		
Lymphatic metastasis			5.391	0.020			6.407	0.011
Yes	26	102			35	93		
No	1	31			2	30		
Stage			4.243	0.039			5.717	0.017
I + II	2	34			3	33		
III + IV	25	99			34	90		
CEA			0.001	0.980			0.009	0.923
Normal	24	118			33	109		
Rise	3	15			4	14		
CA19-9			0.148	0.700			0.091	0.763
Normal	25	120			34	111		
Rise	2	13			3	12		

Table 2 Multivariate analyses of the impact of patient clinicopathological parameters

Index	SE	Wald	df	95%CI	*P*
Tumor site	0.575	1.566	1	0.182–1.731	0.226
T stage	0.864	5.159	1	0.191–5.661	0.024
Lymphatic metastasis	0.661	6.026	1	0.163–2.177	0.013
Clinical stages	0.961	4.026	1	0.091–3.920	0.037
Differentiation	0.927	1.217	1	0.091–3.452	0.305
Size	0.763	2.562	1	0.126–2.503	0.063

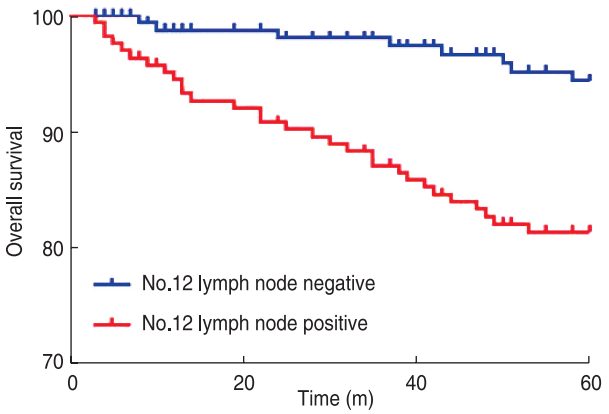

Fig. 2 No.12 Comparison of survival curves between patients in the lymph node-negative and positive groups

lymph node dissection, which greatly reduces the immune ability of patients to tumors and affects the long-term prognosis of patients. In addition, the anatomy of the hepatoduodenal ligament is complex, and the surgical risk is high. Cleaning this area will significantly improve the occurrence of postoperative complications such as bile leakage, gallbladder injury, hepatic artery stenosis, portal vein injury, and lymphoma. Therefore, there is still controversy regarding whether No.12 lymph nodes should be routinely cleaned in radical gastrectomy. However, in this study, combined with the results of routine pathological examination and micrometastasis detection, it was found that the metastasis rate of No.12 lymph nodes could be as high as 23.1%, which proved the necessity of cleaning No.12 lymph nodes during radical gastrectomy.

Feng *et al.* [11] reported that the depth of tumor invasion and Borrmann classification are the most important factors affecting No.12 lymph node metastasis, which is consistent with the conclusion of this study. It further shows that tumor infiltration into the serosa and Borrmann type IV are important factors for lymph node metastasis of gastric cancer No.12. This suggests that patients with poor Borrmann classification, lymph node metastasis in other groups, and late clinical stage should pay more attention to the significance of No.12 lymph node dissection. However, no correlation was observed between No.12 lymph node metastasis and tumor location ($P > 0.05$). The relationship between No.12 lymph node metastasis and tumor location in gastric cancer needs to be further studied.

Regarding the significance of lymph node micrometastasis on the prognosis of patients, some researchers believe that there is a correlation between them, while others believe that micrometastasis has no effect on the prognosis of patients. The patients in this group were followed up for an average of 79.3 months. It was found that the survival time of patients in No.12 lymph node negative group and positive group were (67.3 ± 2.5) months and (28.4 ± 5.4) months respectively. The survival time of patients in the No.12 lymph node-negative group was significantly longer than that in the positive group. This more intuitively illustrates the impact of No.12 lymph node metastasis on patient prognosis. Therefore, we believe that it is necessary to perform No.12 lymph node metastasis in patients with gastric cancer. As a relatively controllable factor, postoperative complications should follow the principle of No.12 lymph node dissection to perform vascular choroidization dissection to avoid the shedding and planting of tumor cells. Careful identification of duct structures, such as the bile duct, portal vein, and hepatic artery, is an important measure to prevent postoperative complications.

In conclusion, No.12 lymph node metastasis is a strong indicator of poor prognosis. Standardized lymph node dissection is recommended for patients with advanced gastric cancer who can undergo radical resection.

Acknowledgments

Not applicable.

Funding

This study was supported by a grant from the Hebei Medical Science Research Project (No. 20191831).

Conflicts of interest

The authors indicated no potential conflicts of interest.

Author contributions

Not applicable.

Data availability statement

Not applicable.

Ethical approval

This study was approved by Handan People's Hospital ethics committee (SWYX:No. 2020-107).

References

1. Zhou Y, Zhang GJ, Wang J, et al. Current status of lymph node micrometastasis in gastric cancer. Oncotarget. 2017;8(31):51963-51969.
2. Liang H. The Precised Management of Surgical Treatment for Gastric Cancer: Interpretation of the 5th edition of Japanese Gastric Cancer Treatment Guideline and the 15th edition of Japanese Classification for Gastric Cancer. Zhonghua Zhong Liu Za Zhi. 2019;41(3):168-172.
3. Dang XD, He Y, Lai BQ. Efficacy of Bispectral index-monitored closed-loop targeted-controlled infusion of propofol for laparoscopic radical operation for gastric cancer. J Hainan Med Univ. 2019;25(1): 58-62.
4. Shen S, Cao S, Jiang H, et al. The short-term outcomes of gastric cancer patients based on a proposal for a novel classification of perigastric arteries. J Gastrointest Surg. 2020;24(11):2471-2481.
5. Lou GC, Dong J, Du J, et al. Clinical significance of lymph node micrometastasis in T1N0 early gastric cancer. Math Biosci Eng. 2020;17(4):3252-3259.
6. Tavares A, Wen X, Maciel J, et al. Occult tumour cells in lymph nodes from gastric cancer patients: should isolated tumour cells also be considered? Ann Surg Oncol. 2020;27(11):4204-4215.
7. Zhang P, Lan TH, Zhou YM, et al. Risk factor analysis of perioperative complications in patients with radical gastrectomy for gastric cancer. Zhonghua Wei Chang Wai Ke Za Zhi (Chinese). 2019;22(8):736-741.
8. Wang JW, Chen CY. Prognostic value of total retrieved lymph nodes on the survival of patients with advanced gastric cancer. J Chin Med Assoc. 2020;83(8):691-692.
9. Takeuchi M, Takeuchi H, Kawakubo H, et al. Risk factors for lymph node metastasis in non-sentinel node basins in early gastric cancer: sentinel node concept. Gastric Cancer. 2019;22(1):223-230.
10. Shimada A, Takeuchi H, Nishi T, et al. Utility of the one-step nucleic acid amplification assay in sentinel node mapping for early gastric cancer patients. Gastric Cancer. 2020;23(3):418-425.
11. Feng JF, Huang Y, Liu J, et al. Risk factors for No. 12p and No. 12b lymph node metastases in advanced gastric cancer in China. Ups J Med Sci. 2013;118(1):9-15.

DOI 10.1007/s10330-021-0526-6
Cite this article as: Dong TZ, Zhang LR. Analysis of the adverse reactions of atezolizumab: a real-world study based on FAERS database. Oncol Transl Med. 2022;8(3):115–120.

Oncology and Translational Medicine
DOI 10.1007/s10330-021-0536-6

June 2022, Vol. 8, No. 3, P121–P125

ORIGINAL ARTICLE

Effects of rearranged during transfection mutation on calcitonin and procalcitonin expression in sporadic medullary thyroid carcinoma*

Yaqiong Ni, Wei Yao, Yunsheng Wang, Hui Wang, Qinjiang Liu (✉)

Department of Head and Neck Surgery, Gansu Provincial Cancer Hospital, Lanzhou 730050, China

Abstract

Objective The aim of this study was to investigate the effects of rearranged during transfection (*RET*) mutation on the expressions of calcitonin (CTn) and procalcitonin (PCT) in sporadic medullary thyroid carcinoma (SMTC).

Methods *RET* mutation was detected by polymerase chain reaction direct sequencing in 64 cases of SMTC, and the expression levels of CTn and PCT in SMTC tissues were detected using the immunohistochemical streptavidin-perosidase (SP) method. The effect of *RET* mutations on the expression of CTn and PCT along with its relationship with clinicopathological parameters were analyzed.

Results The expression rates of CTn and PCT in SMTC tissues were 90.6% (58/64) and 67.2% (43/64), respectively. CTn and PCT expression were found to be associated with tumor size and lymph node metastasis ($P < 0.05$) but not with gender, age, or tumor capsule invasion ($P > 0.05$). There was a significant correlation between CTn and PCT expression ($r = 0.269$, $P = 0.041$), and the intensity of positive CTn expression was positively correlated with *RET* mutation ($r = 0.507$, $P = 0.000$). However, PCT expression was not associated with *RET* mutation ($r = 0.188$, $P = 0.136$).

Conclusion High expression of CTn and PCT was associated with the progression of medullary carcinoma, and the intensity of CTn expression was associated with *RET* mutation. PCT may provide valuable information for the diagnosis and prognosis of SMTC.

Received: 11 November 2021
Revised: 21 December 2021
Accepted: 5 March 2022

Key words: sporadic medullary thyroid carcinoma (SMTC); procalcitonin; calcitonin: rearranged during transfection (*RET*)

Medullary thyroid carcinoma (MTC) is derived from thyroid parafollicular cells and occurs in two forms, namely sporadic (SMTC) and hereditary (HMTC). MTC accounts for approximately 5%–10% of thyroid cancer cases [1], with a high degree of malignancy characterized by high invasiveness and high risks of metastasis, recurrence, and poor prognosis. Thus, early diagnosis is extremely important. The most common tumor marker used for MTC diagnosis and monitoring is calcitonin (CTn) [2–3]. Procalcitonin (PCT) is a precursor of CTn and has been used as a diagnostic marker for bacterial or fungal infections and sepsis [4–5], but recent studies have shown that serum PCT detection is also useful in MTC diagnosis and follow-up [6]. In this study, rearranged during transfection (*RET*) mutations and their effects on the expression of CTn and PCT in patients with SMTC were analyzed. The results were then comprehensively evaluated in reference to clinicopathological parameters to provide valuable information for SMTC diagnosis and treatment.

Materials and methods

Subjects

Data on 64 patients with pathologically confirmed SMTC who were treated at the Department of Head and Neck Surgery, Gansu Cancer Hospital, from October 2007 to January 2018 were collected. Of these, 30 were males and 34 were females, with a median age of 49.8 ± 12.6 years. Thirty-seven patients had lymph node metastasis, while 27 were without lymph node metastasis. All histopathological diagnoses were reconfirmed by two senior pathologists. No patient received treatment for SMTC before being treated at our hospital, and informed

✉ Correspondence to: Qinjiang Liu. Email: liuqj99@126.com
* Supported by a grant from the Gansu Provincial Funding for Health Research (No. GSWSKY2018-13).

Table 1 PCR amplification primers for *RET* mutation

Gene	Sequence (5'→3')	Annealing Temperature
RET ex8	Forward TGCTGCCCTGGGTCTGTC	59 °C
	Reverse ACCTTCCCAAGTCCAGAGTGAATC	
RET ex10	Forward CATGGCTTCAGAAAGGCACTG	59 °C
	Reverse CCTTGTTGGGACCTCAGATGTG	
RET ex11	Forward CATGCTCGATGGGGTGTTC	60 °C
	Reverse GACCCTCACCAGGATCTTGAA	
RET ex13	Forward CTGCTCTGTGCTGCATTTCA	58 °C
	Reverse GCCCCTCTGATGGAAAGTGAC	
RET ex14	Forward GGAGGCAGAGAGCAAGTGGTT	58 °C
	Reverse CCATATGCACGCACCTTCATCT	
RET ex15	Forward CGACTCGTGCTATTTTTCCTC	60 °C
	Reverse AGGCTGAGCGGAGTTCTAAT	
RET ex16	Forward CTCCAGCCCCTTCAAAGATGT	60 °C
	Reverse CCATTTGCCTCACGAACACA	

consent was obtained from all patients and their families.

Reagents and methods

DNA extraction and purification E.Z.N.A.™ FFPE DNA Kit was purchased from Omega Bio-tek (USA), and Green Tag Mix was purchased from Nanjing Vazyme Biotech Co., Ltd. (China). Mouse anti-human PCT monoclonal antibody was purchased from Novus (USA), and CTn antibody, SP immunohistochemical kit, DAB chromogenic kit, phosphate-buffered solution (PBS), and citric acid repair solution were purchased from Beijing Zhongshan Jinqiao Biotechnology Company (China). The primers corresponding to the target fragment of the *RET* gene to be amplified were designed using Primer 5.0 and Oligo6 software (Table 1) and synthesized by Suzhou Jinweizhi Biotechnology Company (China).

All specimens were fixed in 4% neutral formaldehyde, dehydrated, embedded in paraffin, and cut into 4 μm-thick sections. Immunohistochemical staining was performed after reexamination of routine hematoxylin and eosin (HE)-stained sections to verify and determine the diagnosis. Known sections were used as positive controls, and PBS, instead of primary antibody, was used as negative controls. All steps were performed in strict accordance with the instructions provided by the manusfacturer of the SP immunohistochemical kit. After immunohistochemical staining, additional – three to eight sections (4–10 μm thick) were processed with conventional xylene and absolute ethanol, after which DNA was extracted and purified using an E.Z.N.A.™ FFPE DNA Kit according to the manufacturer's instructions. The concentration and purity of the extracted DNA were determined using an ultramicro spectrophotometer. Amplified gene fragments were then determined according to the complete *RET* gene sequence published in the GenBank database of the National Center for Biotechnology Information. Qualified genomic DNA was amplified using polymerase chain reaction, and the products were then sequenced. The sequencing results were compared with the normal *RET* gene sequence to determine whether mutation had occurred. All samples were divided into the mutant and wild-type *RET* groups.

Determination of results

CTn- and PCT-positive products were localized in the cytoplasm or nucleus and were brown and brownish-yellow in color. The results of pathological staining were determined by two professional pathologists with reference to the literature (7). The following scores were given according to the degree of positive staining of the cells: 0, no staining; 1, yellow (+); 2, brownish-yellow (++); and 3, brown (+++). Meanwhile, the following scores were given according to the number of positive cells: 0, positive cell count below 5%; 1, positive cell count below 25% (+); 2, positive cell count ≥ 25% but < 50% (++); and3, positive cell count ≥ 50% (+). Five fields were randomly selected, and 100 cells were counted by light microscopy at 200× magnification, and the average was calculated. The staining degree score and the percentage of stained cells in each slide were multiplied, and a final score of 0 represents a negative while ≥ 1 is a positive.

Statistical analysis

Data analysis was conducted using SPSS 22.0 (SPSS Inc., USA). The correlation of CTn and PCT expressions with clinicopathological parameters was determined using Pearson chi-square (χ^2) test, while that with their *RET* mutations were analyzed by non-parametric Spearman correlation analysis. $|r| \in [0.1, 1]$ was considered correlated, and $P < 0.05$ was considered statistically significant.

Results

CTn and PCT expression and correlation

The positive rates of CTn and PCT in SMTC were 90.6% (58/64) and 67.2% (43/64), respectively. The expressions of CTn and PCT in SMTC tissues were positively correlated ($r = 0.269$, $P = 0.041$) and significantly different ($P < 0.05$; Table 2 and Fig. 1).

Relationship between CTn or PCT expression and clinicopathologic parameters

CTn e xpression was not associated with gender, age, or capsular invasion ($P > 0.05$) but was significantly associated with tumor size ($P = 0.001$) and lymph node metastasis ($P = 0.032$). Meanwhile, PCT expression was not associated with gender, age, tumor size, or capsular invasion but was associated with lymph node metastasis ($P = 0.026$; Table 3)

Table 2 Relationship between CTn and PCT expression in SMTC tissues [*n* (%)]

PCT	CTn			*r*	*P*
	+	++	+++		
<1 (–)	11 (64.7)	5 (29.4)	1 (5.9)	0.269	0.041
≥1 (+)	16 (39.0)	14 (34.1)	11 (26.8)		

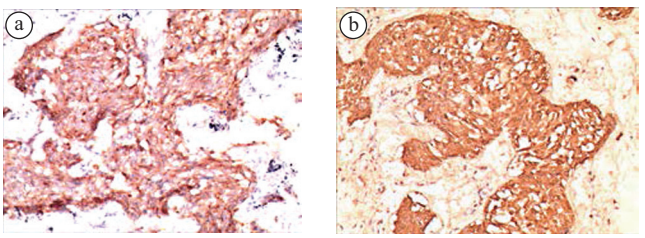

Fig. 1 Immunohistochemical staining of CTn and PCT in SMTC tissues (SP × 200). (a) CTn was positively expressed in SMTC tissues; (b) PCT was positively expressed in SMTC tissues

Relationship between CTn or PCT expression and RET gene mutation

The *RET* mutation rate in SMTC tissues was 37.5% (24/64), with 24 cases in the mutation group and 40 cases in the wild-type group.

Among the *RET* mutants, the proportion of moderate and strong positive CTn expression were 54.2% (13/24) and 33.3% (8/24), respectively, which were higher than the 15.0% (6/40) and 10.0% (4/40) observed in the wild-type. The intensity of positive CTn expression was significantly and positively correlated with *RET* mutation ($r = 0.507$, $P = 0.000$).

The positive rate of PCT in mutant *RET* was 75.0% (18/24), which was higher than the 62.5% (25/40) observed in the wild-type, although the difference was not statistically significant ($P > 0.05$). In addition, no correlation was found between PCT expression and *RET* mutation ($r = 0.188$, $P = 0.136$; Fig. 2 and Table 4).

Discussion

With the development of tumor molecular biology research in recent years, significant achievements have been made in the study of the molecular biology of MTC, particularly for serial studies related to the *RET* gene. *RET* gene mutation detection is of great value in MTC diagnosis, treatment, and prognostic evaluation [8–9].

Table 3 Relationship between CTn or PCT expression and clinicopathological parameters [*n* (%)]

Variables	CTn positive	χ^2	*P*	PCT positive	χ^2	*P*
Gender		0.488	0.485		0.007	0.934
male	28 (93.3)			20 (66.7)		
female	30 (88.2)			23 (67.6)		
Age (years)		0.717	0.397		2.430	0.119
< 55	39 (92.9)			31 (73.8)		
≥ 55	19 (86.4)			12 (54.5)		
Tumor size (cm)		13.094	0.001		0.345	0.842
< 2	6 (60.0)			6 (60.0)		
2–4	23 (95.8)			16 (66.7)		
≥ 4	29 (96.7)			21 (70.0)		
Lymph node metastasis		4.596	0.032		4.982	0.026
N0	22 (81.5)			14 (51.9)		
N1	36 (97.3)			29 (78.4)		
Capsular invasion		0.003	0.955		0.015	0.902
Yes	38 (90.5)			28 (66.7)		
No	20 (90.9)			15 (68.2)		

MTC has high malignancy, poor prognosis, and is prone to metastasis and recurrence; thus, its early diagnosis is crucial. This highlights the importance of valuable molecular markers that may help advance early diagnosis and prognostic evaluation of MTC.

CTn, a 32-amino acid short peptide hormone synthesized and secreted by thyroid C cells, is the product of the CALC1 gene and the main tumor marker of MTC. It is currently widely used for MTC diagnosis and follow-up [10–11]. While most of the CTn tests in clinical work use serological test values to assess disease progression, postoperative follow-up, and prognosis, they can also be used to guide the choice of surgical approach for MTC [12]. The results of this study showed that the positive rate of CTn in SMTC tissues was 90.6% and that its expression was related to tumor size and lymph node metastasis, similar to the serum detection results of CTn values [13–14]. The expression of CTn in tumor tissues also showed an increasing trend with the progression of the disease, and the probability of cervical lymph node metastasis increased upon CTn expression. Although the level of CTn expression in MTC tissues is similar to that of serum CTn, the latter is affected by hypercalcemia, hypergastrinemia, and other chronic autoimmune diseases [15]. The expression status of CTn in tumor tissues

Table 4 Relationship between CTn or PCT expression and *RET* mutation [*n* (%)]

RET	CTn expression				χ^2	*P*	*r*	*P*	PCT expression				χ^2	*P*	*r*	*P*
	+++	++	+	-					+++	++	+	–				
mutant	8 (33.3)	13 (54.2)	1 (4.2)	2 (8.3)	25.309	0.000	0.507	0.000	14 (58.3)	4 (16.7)	0	6 (25.0)	2.627	0.269	0.188	0.136
wild-type	4 (10.0)	6 (15.0)	26 (65.0)	4 (10.0)					15 (37.5)	10 (25.0)	0	15 (37.5)				

can directly reflect the synthesis of CTn by tumors, which can in turn reflect tumor growth. This study showed that the intensity of positive CTn expression intensity was positively correlated with *RET* mutation and that the proportions of moderate and strong positive CTn in the mutant *RET* group were significantly higher than those in the wild-type *RET* group ($P = 0.000$). Mutation of *RET* led to abnormal structure and function of some proteins or enzymes in the body, resulting in uncontrolled cell growth and tumorigenesis while increasing CTn mRNA, followed by increased CTn synthesis and secretion. A stronger CTn expression indicated a higher degree of malignancy and poor prognosis of the tumor, while the clinical manifestations of the patients were characterized by rapid disease progression, poor therapeutic efficacy, and poor prognosis.

PCT is a polypeptide containing 116 amino acids composed of CTn and a product of the CALC1 gene. In thyroid C cells, transcription and synthesis generate pre-mRNA, which is then translated by polypeptidase to form PCT [16]. PCT, as a specific indicator for the differential diagnosis between infectious and noninfectious diseases, has also been reported to be expressed at increased levels in MTC and is considered a valuable tumor marker for MTC diagnosis and follow-up [17–18]. Therefore, serum PCT testing has been recommended as a routine test for MTC; however, there are many influencing factors of PCT in the serum, and its clinical value is limited [19]. This study showed that the positive expression level of PCT in SMTC tissues was associated with lymph node metastasis, similar to that reported in serum PCT studies [6, 18], reinforcing the value of PCT in the diagnosis and prognostic evaluation of MTC. Previous studies have also suggested a correlation between PCT and CTn levels in the serum of patients with MTC. PCT is relatively stable compared with serum CTn under *in vitro* conditions and in some cases of patients with MTC and negative serum CTn or low CTn levels. A low PCT to CTn ratio may indicate that it is related to C cell proliferation, while a high ratio is related to MTC metastasis [20–21]. In this study, we found a significant correlation between PCT and CTn expression in SMTC tissues ($P = 0.041$), whereas no correlation was observed between PCT expression and *RET* mutation ($r = 0.188$, $P = 0.136$). This suggests that PCT expression is relatively stable in SMTC tissues and may be a valuable and reliable indicator for MTC diagnosis.

To conclude, CTn and PCT were highly expressed in SMTC tissues and were correlated with tumor size and lymph node metastasis. Their expression was significantly correlated, suggesting that they are associated with tumor occurrence and development. We believe that PCT expression in MTC tissues may be used as a diagnostic indicator and as a reference indicator to evaluate the degree of malignancy and prognosis of MTC. However, the relationship between PCT expression in MTC tissues and serum PCT levels and the significance of changes in serum PCT require further exploration.

Acknowledgments
Not applicable.

Funding
This study was supported by a grant from the Gansu Provincial Funding for Health Research (No. GSWSKY2018-13).

Conflicts of interest
The authors indicated no potential conflicts of interest.

Author contributions
Not applicable.

Data availability statement
Not applicable.

Ethical approval
Not applicable.

References

1. Mohammadi M, Hedayati M. A brief review on the molecular basis of medullary thyroid carcinoma. Cell J. 2017;18(4):485-492.
2. Bae YJ, Schaab M, Kratzsch J. Calcitonin as biomarker for the medullary thyroid carcinoma. Recent Results Cancer Res. 2015;204:117-137.
3. van Veelen W, de Groot JW, Acton DS, et al. Medullary thyroid carcinoma and biomarkers: past, present and future. J Intern Med. 2009;266(1):126-140.
4. Hou XF, Liu QJ, Tian YX. Effect of parathyroid hormone on apoptosis of human medullary thyroid carcinoma cells. Oncol Transl Med. 2017; 3(6):241-244.
5. Charles PE, Kus E, Aho S, et al. Serum procalcitonin for the early recognition of nosocomial infection in the critically ill patients: a preliminary report. BMC Infect Dis. 2009 Apr 22;9:49.
6. Trimboli P, Seregni E, Treglia G, et al. Procalcitonin for detecting medullary thyroid carcinoma: a systematic review. Endocr Relat Cancer. 2015;22(3):R157-164.
7. Brunello AG, Weissenberger J, Kappeler A, et al. Astrocytic alterations in interleukin-6/Soluble interleukin-6 receptor alpha double-transgenic mice. Am J Pathol. 2000;157(5):1485-1493.
8. Mohammadi M, Hedayati M. A brief review on the molecular basis of medullary thyroid carcinoma. Cell J. 2017;18(4):485-492.
9. Accardo G, Conzo G, Esposito D, et al. Genetics of medullary thyroid cancer: An overview. Int J Surg. 2017;41 Suppl 1:S2-S6.
10. Findlay DM, Sexton PM. Calcitonin. Growth factors. 2004;22(4):217-224.
11. Felsenfeld AJ, Levine BS. Calcitonin, the forgotten hormone: does it deserve to be forgotten? Clin Kidney J. 2015;8(2):180-187.
12. Song NN, Wang YZ, Li X, et al. Study on calcitonin in diagnosis and surgery selection in patients with medullary thyroid cancer. J Tianjin

Med Univ (Chinese). 2017;3:61-63.
13. Yip DT, Hassan M, Pazaitou-Panayiotou K, et al. Preoperative basal calcitonin and tumor stage correlate with postoperative calcitonin normalization in patients undergoing initial surgical management of medullary thyroid carcinoma. Surgery. 2011;150(6):1168-1177.
14. Saltiki K, Rentziou G, Stamatelopoulos K, et al. Small medullary thyroid carcinoma: post-operative calcitonin rather than tumour size predicts disease persistence and progression. Eur J Endocrinol. 2014;171(1):117-126.
15. Guesgen C, Willms A, Zwad A, et al. Investigation of factors potentially influencing calcitonin levels in the screening and follow-up for medullary thyroid carcinoma: a cautionary note. BMC Clin Pathol. 2013;13(1):27.
16. Davies J. Procalcitonin. J Clin Pathol. 2015;68(9):675-679.
17. Bihan H, Becker KL, Snider RH, et al. Calcitonin precursor levels in human medullary thyroid carcinoma. Thyroid. 2003;13(8):819-822.
18. Karagiannis AK, Girio-Fragkoulakis C, Nakouti T. Procalcitonin: A new biomarker for medullary thyroid cancer? A systematic review. Anticancer Res. 2016;36(8):3803-3810.
19. Algeciras-Schimnich A, Preissner CM, Theobald JP, et al. Procalcitonin: a marker for the diagnosis and follow-up of patients with medullary thyroid carcinoma. J Clin Endocrinol Metab. 2009;94(3):861-868.
20. Kaczka K, Mikosiński S, Fendler W, et al. Calcitonin and procalcitonin in patients with medullary thyroid cancer or bacterial infection. Adv Clin Exp Med. 2012;21(2):169-178.
21. Walter MA, Meier C, Radimerski T, et al. Procalcitonin levels predict clinical course and progression-free survival in patients with medullary thyroid cancer. Cancer. 2010;116(1):31-40.

DOI 10.1007/s10330-021-0536-6
Cite this article as: Ni YQ, Yao W, Wang YS, et al. Effects of RET mutation on CTn and PCT expression in sporadic medullary thyroid carcinoma. Oncol Transl Med. 2022;8(3):121–125.

Oncology and Translational Medicine
DOI 10.1007/s10330-021-0507-7

June 2022, Vol. 8, No. 3, P126–P134

ORIGINAL ARTICLE

Effects of long non-coding RNA GAS5 on proliferation and apoptosis of hepatocellular carcinoma cells through miR-26a-5p action

Zunli Yi[1] (✉), Xiaoguang Guo[2], Xianxue Jiang[3], Fengmei Luo[4]

[1] Pathology Department, Yuechi People's Hospital, Guangan 638300, China
[2] Pathology Department, Nanchong Central Hospital, Nanchong 637000, China
[3] The First Department of General Surgery, Yuechi People's Hospital, Guangan 638300, China
[4] The Second Department of General Surgery, Yuechi People's Hospital, Guangan 638300, China

Abstract

Objective Long non-coding RNAs (lncRNAs) regulate tumor development and progression by promoting tumor proliferation, invasion, and metastasis. The aim of the study was to investigate the effects of lncRNA growth arrest-special 5 (GAS5) on proliferation and apoptosis of hepatocellular carcinoma (HCC) cells through miR-26a-5p action.

Methods Expression levels of GAS5 were detected in cancerous and paracancerous tissue of 80 HCC patients by RT-qPCR. The starBase tool predicted that GAS5 had binding sites for the miRNA miR-26a-5p, which was also highly expressed in HCC tissue. The relationship between GAS5 and miR-26a-5p was confirmed using a luciferase reporter assay. The role of these lncRNAs was further explored by transfecting plasmids into SMMC-7721 cells and classifying the cells as follows: NC group, GAS5 group, anti-miR-26a-5p group, and GAS5 + miR-26a-5p group. Cell proliferation, cell cycle, and apoptosis were detected in each group. The relationship between miR-26a-5p and phosphatase and tensin homolog deleted on chromosome 10 (PTEN) was analyzed by TargetScan database prediction and luciferase reporter assay. Western blotting was used to quantify PTEN, phosphatidylinositol 3-kinase (PI3K), phosphorylated protein kinase B (p-Akt), cyclin D1, and human P27 protein (P27).

Results GAS5 was downregulated, while miR-26a-5p was upregulated in HCC tissue compared to in paracancerous tissue. High GAS5 levels and low miR-26a-5p levels inhibited cell proliferation, increased the number of G0/G1 phase cells, promoted cell apoptosis, promoted PTEN and P27 expression, and inhibited PI3K, P-Akt, and cyclin D1 expression at the protein level. Upregulation of miR-26a-5p attenuated the effects of GAS5 upregulation on the proliferation, cell cycle, and apoptosis of HCC cells and on the expression of PTNE/PI3K/Akt signaling pathway-related proteins.

Conclusion Low GAS5 levels regulate the proliferation and apoptosis of HCC cells via the PTNE/PI3K/Akt signaling pathway and are linked to upregulation of miR-26a-5p.

Received: 7 July 2021
Revised: 23 November 2021
Accepted: 2 May 2022

Key words: lncRNA GAS5; miR-26a-5p; hepatocellular carcinoma (HCC); cell proliferation; cell cycle; apoptosis

Primary liver cancer is one of the most common malignant tumors, with an incidence second only to that of lung cancer worldwide [1]. Approximately half of liver cancer patients globally are from China, and approximately 350 000 people die of liver cancer every year, posing a serious threat to the health of Chinese individuals [2]. Hepatocellular carcinoma (HCC) has the highest incidence in primary liver cancers. HCC is characterized by high malignancy and more invasive growth and occurs when cancer cells invade the arteriovenous system and bile ducts. HCC has a low surgical resection rate and frequent recurrence and metastasis after surgery, which seriously affects the survival rate of HCC patients [3]. Recent studies have found that long noncoding RNA (lncRNA) plays an important role in the regulation of the cell cycle, tumor cell invasion and metastasis, dose compensation

✉ Correspondence to: Zunli Yi. Email: YZL1575@163.com

effects, and other biological behaviors and are therefore similar to oncogenes or tumor suppressor genes. The lncRNA small nucleolar RNA growth arrest-special 5 (GAS5) is located at the break point of human 6q15 chromosome translocation. GAS5 plays a role in many cancers, including cervical [4], stomach [5], and prostate cancer [6]. Many tumor suppressor genes, oncopromoter genes, non-coding RNAs, microRNA (miRNA), and protein factors have been implicated in the occurrence and development of HCC. MiR-26a-5p is lowly expressed in HCC cells, and up-regulation of its expression can inhibit the proliferation and invasion of HCC cells and promote cancer cell apoptosis [7]. The expression of miR-21 is up-regulated in HCC, while the expression of PTEN is down-regulated. Up-regualation of miR-21 promotes the proliferation, migration and invation of HCC cells by inhibiting the expression of PTEN [8]. But the role of GAS5 in HCC remains unclear. A variety of microRNA-lncRNA interactions are also involved in the occurrence and development of cancer. GAS5 inhibited the proliferation and invasion ability of HCC cells and promoted HCC cell apoptosis by targeting down-regulation of miR-1323 expression [9]. GAS5 inhibits the proliferation of laryngeal squamous cell carcinoma cells and promotes autophagy in cancer cells by targeting down-regulation of miR-26a-5p expression [10]. Therefore, in the present study, we explored the effects of GAS5 and miR-26a-5p on HCC cell cycle and apoptosis, and analyzed their targeted regulatory roles, may identify novel targets for HCC treatment in future.

Materials and methods

Samples and participants

Cancer and normal tissue samples (more than 2.5 cm away from the cancer tissue) were obtained from 80 patients with HCC who received surgical treatment in our hospital (Yuechi People's Hospital, Guangan, China) from July 2018 to October 2019. All cases were pathologically confirmed to be primary HCC without other primary tumors. This study was approved by the Ethics Committee of our hospital (Yuechi People's Hospital, Guangan, China), with voluntary participation and signed informed consent obtained from the patients and their families. Human hepatocyte *LO2* and human HCC cell lines (*HepG2.2.15, SMMC-7721, Huh7, Bel-7402, MHCC97-H,* and *MHCC97-L*) were purchased from Shanghai Cell Bank at the Chinese Academy of Sciences.

Reagents and instruments

Cell transfection plasmids were purchased from Shanghai Jima Co., Ltd, China. Dulbecco's modification of Eagle's medium (DMEM) and fetal bovine serum were purchased from Gibco, USA. The reverse transcription kit was purchased from Sigma, USA. Lipofectamine-2000 was purchased from Vector, Inc., USA. Trizol reagent was purchased from TAKARA, Japan. The EdU cell proliferation kit was purchased from Guangzhou Ruibo, China. The apoptosis detection kit and cell cycle detection kit were purchased from Shanghai Biyuntian Biotechnology, China. The western blotting kit was purchased from BD, USA. Rabbit polyclonal PI3K (AB39670), rabbit monoclonal Bax (AB32503), rabbit monoclonal Bcl-2 (AB32124), rabbit polyclonal P27 (AB137736), and rabbit monoclonal cyclin D1 (AB16663) were purchased from Abcam, USA. Goat anti-rabbit IgG secondary antibody was purchased from Jinqiao, China. Luciferase assay kit was purchased from Promega, USA.

Prediction of the relationship between miR-26a-5p, GAS5, and PTEN

The bioinformatics tools starBase and TargetScan were used to predict the relationship between miR-26a-5p, GAS5, and PTEN.

RT-qPCR of GAS5 and miR-26a-5p in HCC tissue and cells

Total RNA was extracted using the Trizol reagent according to the manufacturer's instructions. Reverse transcription was performed on 20 ng/μL of total RNA according to the manufacturer's instructions. RNA was reverse transcribed into cDNA by Prime Script™ RT Master Mix. And the quality of RNA was determined by nanodrop. Real time quantitative PCR (RT-qPCR) was performed according to the following program: denaturation at 75 °C for 2 min, followed by 40 cycles of denaturation at 90 °C for 5 min, annealing at 60 °C for 60 s, and extension at 72 °C for 30 s. The relative expression of target mRNAs was determined using the $2^{-\Delta\Delta CT}$ method [10–11]. The experiment was repeated independently three times for each sample.

Cell culture and transfection

The human HCC cell line SMMC-7721 was cultured in DMEM containing 10% fetal bovine serum. The medium was changed once every 2 days, until a confluency of about 90% was reached. SMMC-7721 cells in logarithmic growth phase were transfected using Lipofectamine 2000 according to the manufacturer's instructions. The cells were grouped as follows: the NC group was transfected with a negative control plasmid, the GAS5 group was transfected with an overexpression plasmid for GAS5, the anti-miR-26a-5p group was transfected with an siRNA plasmid for miR-26a-5p, and the GAS5 + miR-26a-5p group was transfected simultaneously with a GAS5 overexpression plasmid and a miR-26a-5p overexpression plasmid.

RNA immunoprecipitation (RIP) assay

RIP was performed using a MagnaRNA immunoprecipitation kit according to the manufacturer's instructions. SMMC-7721 cells were transfected with miR-26a-5p mimic or miR-NC and then collected and lysed in cell lysis buffer from RIP kit. The supernatant was collected and incubated in RIP immunoprecipitation buffer containing magnetic beads bound to Ago2 or IgG antibodies, and the expression level of GAS5 enriched on the beads was analyzed by RT-qPCR.

Luciferase reporter assay

Based on the binding sites predicted by TargetScan, the GAS5 and PTEN fragments containing miR-26a-5p binding sites were amplified by PCR, and the amplified fragments were inserted into the psiCHECK luciferase vector. Wild-type plasmid was constructed for both GAS5 and PTEN and denoted as psiCHECK-GAS5-wild and psiCHECK-PTEN-wild, respectively. Simultaneously, nucleotides in the binding sites were mutated, resulting in the construction of mutant plasmids psiCHECK-GAS5-mutant and psiCHECK-PTEN-mutant. Both miR-26a-5p mimic and negative control mimic-NC were co-transfected with no-load plasmid, psiCHECK-GAS5-wild and psiCHECK-PTEN-wild, or psiCHECK-GAS5-mutant and psiCHECK-PTEN-mutant plasmids. The luciferase activity was detected at 24 h after transfection in HEK293 cells according to the manufacturer's instructions.

EdU assay

Cells in each group were digested with trypsin and then inoculated into 96-well plates at a density of 5 × 10^3 cells/well. Cells were cultured for 24 h and then stained and washed according to the manufacturer's instructions. The cells were photographed and analyzed using a fluorescence inverted microscope (Nikon, Japan). Cell proliferation rate = positive edU staining under field / positive Hochest staining under field × 100%.

Flow cytometry

Adherent cells from each group were removed from their culture dish by trypsinization. Cells were resuspended in binding buffer and gently aspirated into single-cell suspensions. After incubating at 25 °C for 15 min, the rate of apoptosis and the cell cycle stage in each group were determined by flow cytometry. Annexin V-FITC (5 μL) and 7-AAD (5 μL) were added to each group, and the number of cells was adjusted to about 1 × 10^5 cells.

Western blotting

Total protein was extracted from sample tissue and cells using a total protein extraction kit (Biyuntian, China) according to the manufacturer's instructions. Protein content was determined by BCA assay (Biyuntian, China). Protein samples were separated using SDS-PAGE and then transferred to PVDF membrane. Membranes were incubated in blocking solution containing 5% BSA at room temperature for 2 h. Antibody diluents of PTEN (1:500), PI3K (1:2000), P-Akt (1:1000), P27 (1:1000), Cyclin D1 (1:1000) and GAPDH (1:5000) were added and incubated at 4 °C overnight. Membranes were washed with buffer solution three times, and then, the diluted secondary antibody was added. After incubation at room temperature for 1 h, the blot was visualized and analyzed using a chemiluminescent substrate reagents (ECL) and ImageJ software.

Statistical analysis

SPSS version 19.0 was used for statistical analysis, and GraphPad version 5.01 was used to generate figures. Measurement data were expressed as the mean ± standard deviation. Pearson's co-efficient was used for correlation analysis. One-way analysis of variance was used for comparison between multiple groups, and independent sample *t* tests were used for comparison between two groups. A $P < 0.05$ was considered to be statistically significant.

Results

Expression of GAS5 and miR-26a-5p in HCC tissue and cell lines

The expression level of GAS5 and miR-26a-5p in HCC and adjacent paracancerous tissue was detected by RT-qPCR. Compared with that in the adjacent tissue, the expression of GAS5 was significantly decreased in HCC tissue, and the expression of miR-26a-5p was significantly increased ($P < 0.05$). The expression levels of GAS5 and miR-26a-5p in HCC cell lines HepG2.2.15, SMMC-7721, HUH7, Bel-7402, MHCC97-H, and MHCC97-L were significantly different from those in the human hepatocyte cell line LO2 ($P < 0.05$; Fig. 1).

Relationship between GAS5 and miR-26a-5p

The starBase database was used to predict several binding sites between GAS5 and miR-26a-5p (Fig. 2a). A dual luciferase reporter assay was performed to confirm these interactions. The luciferase activity of psiCHECK-GAS5-wild was significantly enhanced after transfection of miR-26a-5p, while the luciferase activity of the psiCHECK-GAS5-mutant and no-loading plasmids did not change significantly ($P > 0.05$; Fig. 2b). This suggests that miR-26a-5p has a targeted regulatory relationship with GAS5. The overexpression of miR-26a-5p resulted in a significantly higher level of RIP Ago2-enriched GAS5, while the enrichment effect of the RIP IgG group was significant (Fig. 2c).

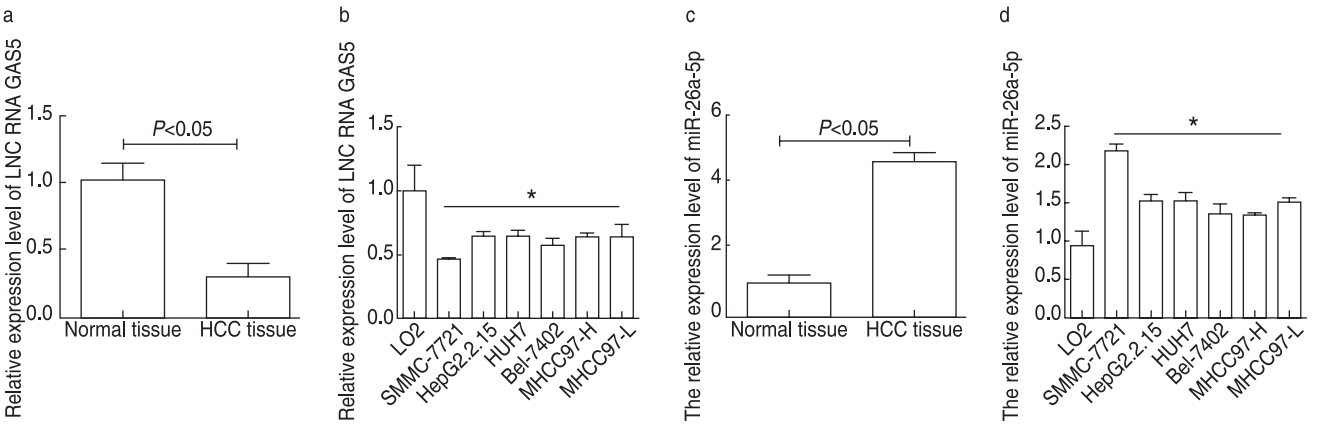

Fig. 1 Quantitation of GAS5 and miR-26a-5p in HCC tissue and cell lines. (a) The expression of GAS5 was detected in HCC and adjacent tissue by RT-qPCR. (b) GAS5 was expressed at low levels in all HCC cell lines but at a high level in a hepatocyte cell line (LO2). (c) The expression of miR-26a-5p was detected in HCC and adjacent tissue by RT-qPCR. (d) miR-26a-5p was expressed at high levels in all HCC cell lines but at a low level in a hepatocyte cell line (LO2). * $P < 0.05$; HCC: hepatocellular carcinoma

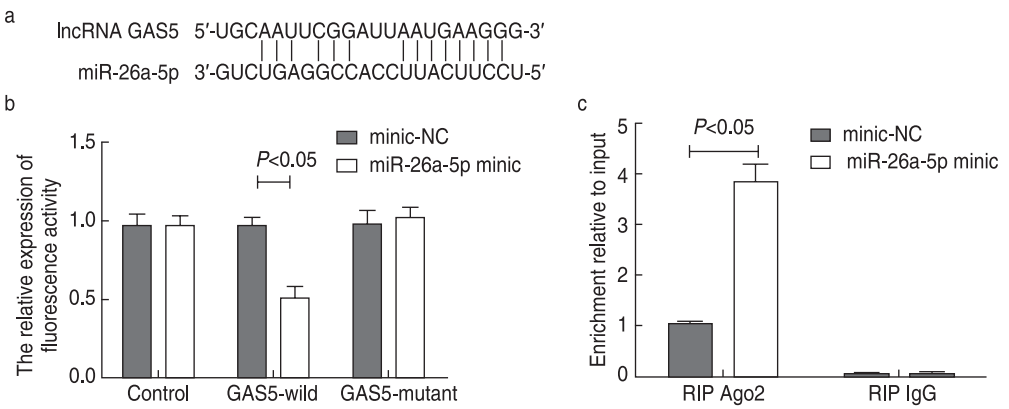

Fig. 2 Relationship between GAS5 and miR-26a-5p. (a) The predicted binding sites of GAS5 and miR-26a-5p. (b) Double luciferase reporter assay to confirm the relationship between GAS5 and miR-26a-5p. (c) RT-qPCR was used to detect RIP Ago2 and RIP IgG-enriched GAS5 levels in SMMC-7721 cells transfected with miR-26a-5p or miR-NC

Effects of GAS5 and miR-26a-5p on the proliferation of SMMC-7721 cells

An EdU assay was used to detect the proliferative ability of cells in each group. There was a statistically significant difference in the number of EdU positive cells between all groups ($P < 0.05$). Pairwise comparison revealed that the GAS5 and anti-miR-26a-5p groups had significantly fewer EdU-positive cells compared to the NC group ($P < 0.05$). The number of EdU positive cells in the lncRNA GAS5 + miR-26a-5p group was significantly higher than that of the GAS5 group ($P < 0.05$; Fig. 3).

Effect of GAS5 and miR-26a-5p on the cell cycle of SMMC-7721 cells

Flow cytometry was used to detect the cell cycle of cells in each group. There was a statistically significant difference in cell cycle phases among all groups ($P < 0.05$). Pairwise comparisons revealed that the number of cells in the G0/G1 phase was significantly higher in the GAS5 and anti-miR-26a-5p groups compared to that in the NC group, while the number of cells in the S-phase was significantly decreased ($P < 0.05$). The number of cells in the G0/G1 phase was significantly lower in the lncRNA GAS5 + miR-26a-5p group compared to that in the GAS5 group, while the number of cells in the S phase was significantly higher ($P < 0.05$; Fig. 4).

Effects of GAS5 and miR-26a-5p on apoptosis in SMMC-7721 cells

There was a statistically significant difference in apoptosis rates among all groups ($P < 0.05$). Pairwise comparisons revealed that the number of apoptotic cells

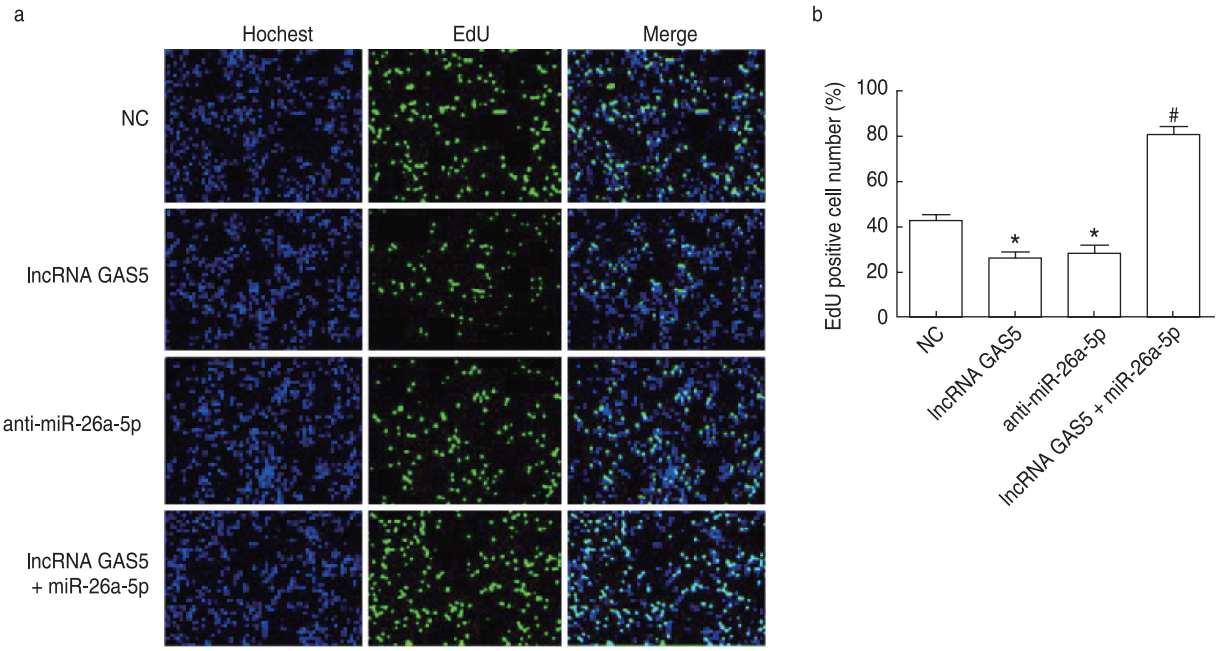

Fig. 3 Proliferative ability of transfected SMMC-7721 cells in each group detected by EdU assay (100×). (a) An EdU assay was used to detect cell proliferation in each group. (b) The number of EdU- positive cells in each group. * $P < 0.05$ compared to the NC group, # $P < 0.05$ compared with the GAS5 group

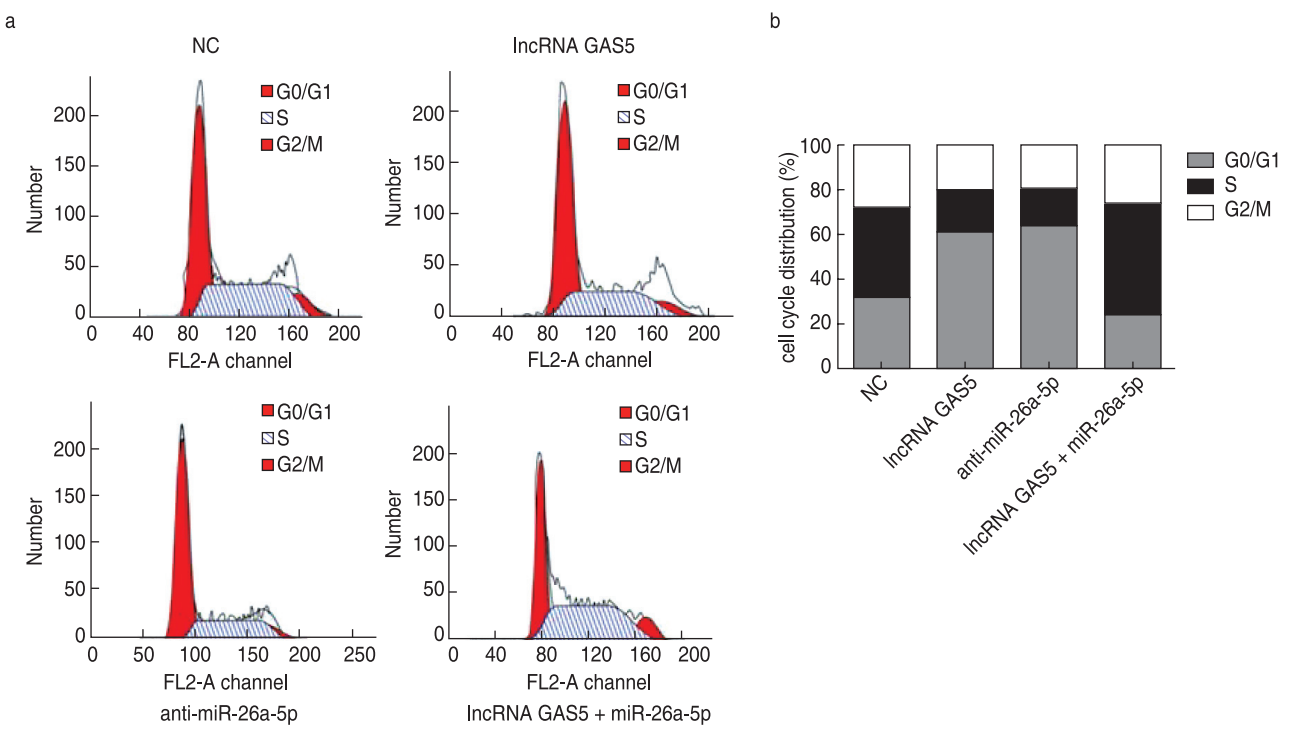

Fig. 4 Cell cycle phase differences in transfected SMMC-7721 cells in each group according to flow cytometry. (a) Flow cytometry results for each group. (b) Cell cycle stage distribution in each group

in the GAS5 and anti-miR-26a-5p groups was significantly higher than in the NC group ($P < 0.05$). The number of apoptotic cells in the lncRNA GAS5 + miR-26a-5p group was significantly reduced compared to in the GAS5 group ($P < 0.05$; Fig. 5),

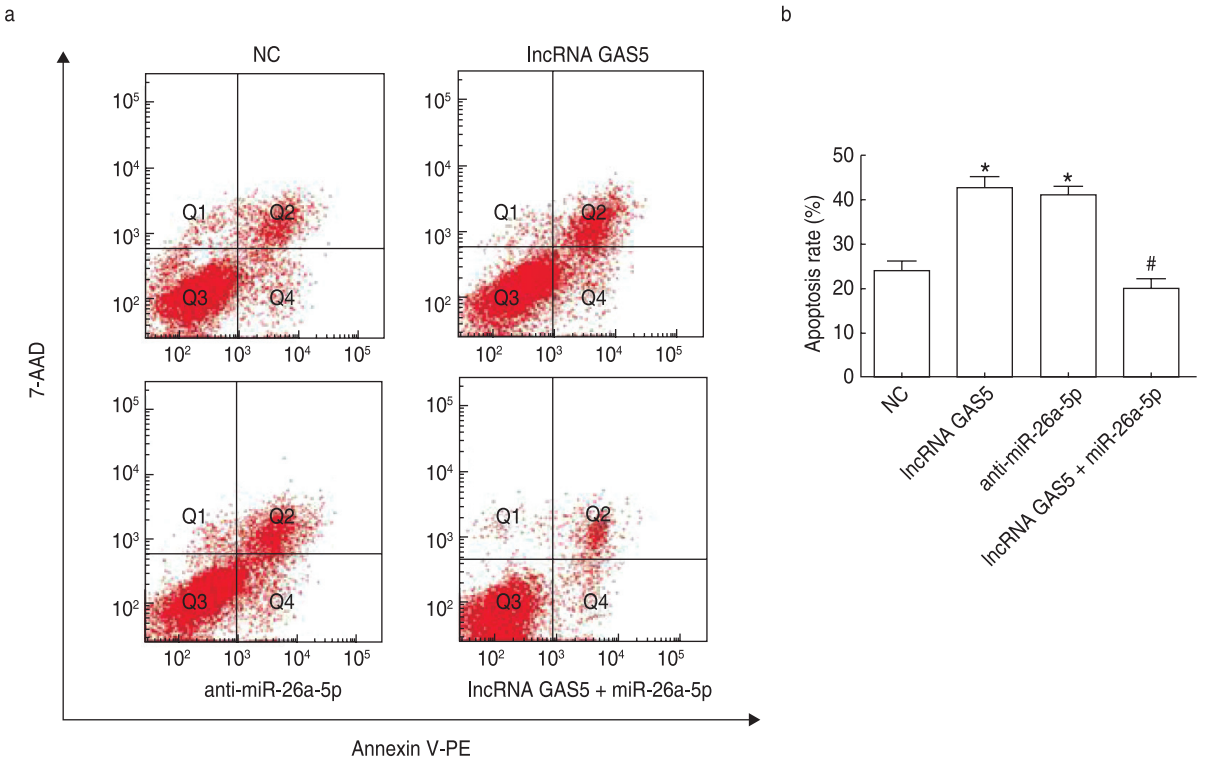

Fig. 5 Apoptosis of SMMC-7721 cells in each group according to flow cytometry. (a) Flow cytometry was used to detect apoptosis in each group. (b) Apoptosis rate in each group. * $P < 0.05$ compared with the NC group, # $P < 0.05$ compared with the GAS5 group

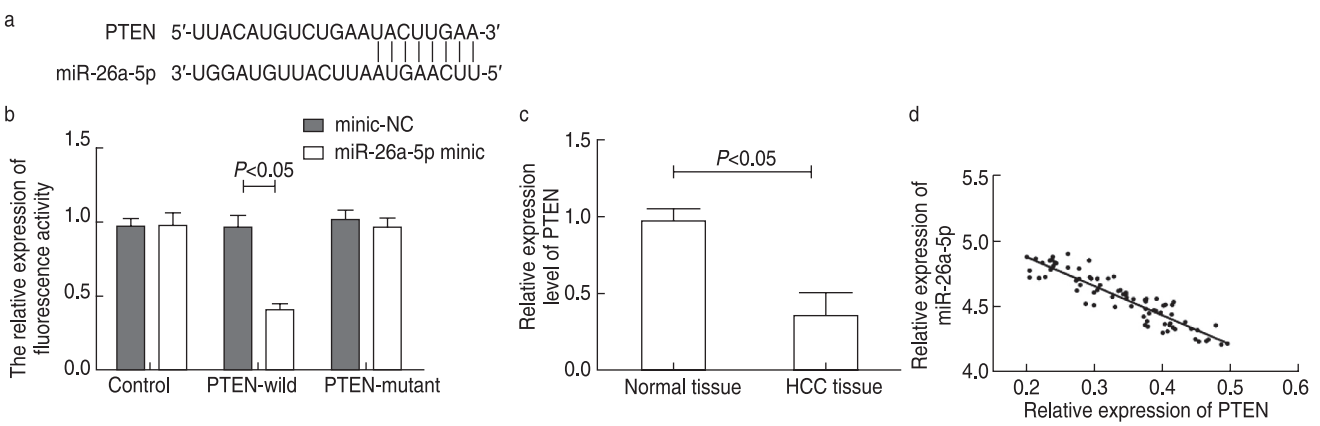

Fig. 6 Relationship between PTEN and miR-26a-5p. (a) Predicted binding site between miR-26a-5p and PTEN. (b) Binding was confirmed by a double luciferase reporter assay. (c) Western blotting was used to detect the expression levels of PTEN in HCC and normal tissue. (d) The level of mir-26a-5p was negatively correlated with the level of PTEN

Relationship between PTEN and miR-26a-5p

TargetScan analysis predicted that miR-26a-5p and PTEN had binding sites (Fig. 6a). A dual luciferase reporter assay showed that the luciferase activity of psiCHECK-PTEN-wild was significantly reduced after transfection with an miR-26a-5p mimic, while the luciferase activity of psiCHECK-PTEN-mutant and no-plasmid did not change significantly ($P > 0.05$; Fig. 6b). This suggests that miR-26a-5p has a regulatory relationship with PTEN protein. The expression of PTEN in HCC tissue was significantly lower than that in the adjacent normal tissue ($P > 0.05$; Fig. 6c). Interestingly, mir-26a-5p levels were negatively correlated with PTEN levels ($r = –0.915$, $P < 0.05$; Fig. 6d).

Western blotting

Western blotting was used to quantify the expression levels of PTEN, PI3K, p-Akt, P27, and cyclin D1 protein in each group. The differences between groups were

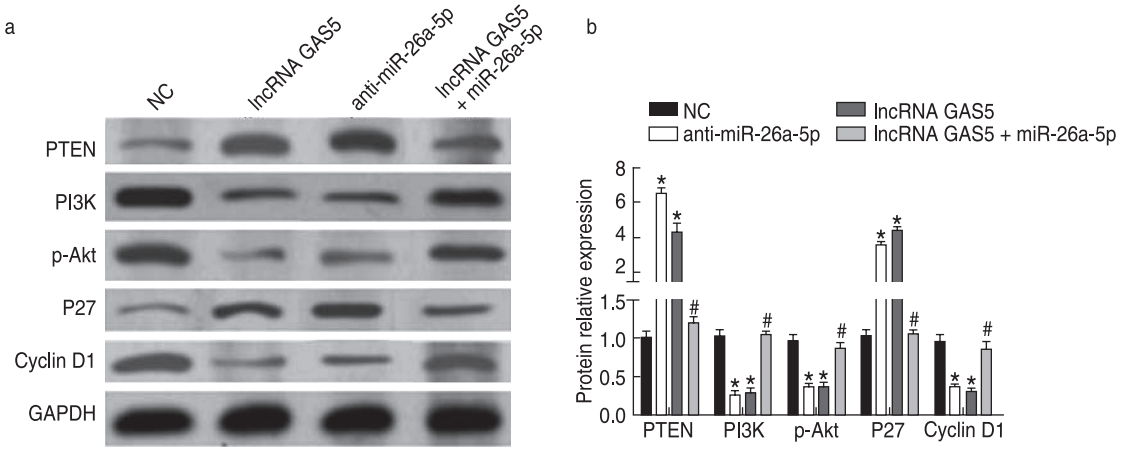

Fig. 7 Apoptosis and cyclin-related protein expression in transfected SMMC-7721 cells in each group according to western blot analysis. (a) Protein bands were detected in each group, (b) Relative protein expression based on densitometry of (a). * $P < 0.05$ compared with the NC group, # $P < 0.05$ compared with the GAS5 group

statistically significant (all $P < 0.05$). The expression of PTEN and P27 was significantly higher in the GAS5 and anti-miR-26a-5p groups than in the NC group, while the expression of PI3K, p-Akt, and cyclin D1 was significantly lower ($P < 0.05$). The expression of PTEN and P27 was significantly lower in the lncRNA GAS5 + miR-26a-5p group than in the GAS5 group, while the expression of PI3K, p-Akt, and cyclin D1 was higher ($P < 0.05$; Fig. 7).

Discussion

The role of lncRNA in cancer is expanding rapidly, with increased research interest in recent years driving important new discoveries. The lncRNA GAS5 can exert pro-cancer or anti-cancer roles in different tumors. For example, Liu *et al* [12] found that downregulation of GAS5 could inhibit the invasion and metastasis of gastric cancer cells by altering the levels of serine-rich spermatogenesis-related protein 2 (SPATS2). However, Song *et al* [13] found that GAS5 was expressed at low levels in colorectal cancer tissue and that overexpression of GAS5 could regulate enhancer of zeste homolog 2 (EZH2) by promoting and regulating enhancer of histone methyltransferase 2 (EHMT2). EZH2 inhibits the invasion and metastasis of breast cancer. However, the role of GAS5 in HCC had not yet been established. Therefore, in the present study, we determined that GAS5 expression was decreased in HCC tissue compared with in the surrounding paracancerous tissue. GAS5 may, therefore, play a tumor suppressive role in HCC. The occurrence of tumors is often accompanied by changes in cell proliferation and growth patterns [14]. To verify the biological role of GAS5 in the development of HCC, we overexpressed GAS5 in the HCC cell line SMMC-7721 and found that overexpression of GAS5 reduced the proliferation of SMMC-7721 cells. Moreover, the number of cells in the G0/G1 phase increased, and the number of apoptotic cells increased. Overexpression of GAS5 could therefore inhibit the proliferation of cancer cells, block the cycle of cancer cells in the G0/G1 phase, and promote the apoptosis of cancer cells.

Previous studies have shown that miRNA binds to target genes through incomplete base complementarity, thus affecting the apoptosis, migration, and metastasis of tumor cells and triggering the necrosis and apoptosis of the surrounding cells [15]. Due to this ability, miRNA is also an important link in the role of lncRNA. In the present study, we used cluster analysis and starBase to predict that miR-26a-5p had binding sites with lncRNA GAS5 and then confirmed that miR-26a-5p was highly expressed in HCC tissue. Previous studies have shown that high levels of miR-26a-5p can promote gastric cancer and that the downregulation of miR-26a-5p plays an important role in blocking the cell cycle in gastric cancer and inducing apoptosis [16]. In the present study, inhibition of miR-26a-5p reduced cell proliferation, arrested cells in the G0/G1 phase, and promoted apoptosis in an HCC cell line. When GAS5 is overexpressed, simultaneous overexpression of miR-26a-5p can reverse the anti-cancer effects of GAS5. These results suggest that GAS5 regulates cell proliferation, cell cycle, and apoptosis by inhibiting the expression of miR-26a-5p, thereby inhibiting the progression of HCC.

A binding site for miR-26a-5p was predicted on PTEN protein using the TargetScan database. Abnormal expression of PTEN protein activates the PTEN/PI3K/Akt signaling pathway, which is one of the most important signal transduction pathways and can regulate the occurrence and development of autoimmune diseases, diabetes, and other diseases. PTEN is an important tumor suppressor gene with abnormal expression in gastric

cancer, colorectal cancer, and other cancers [17]. In normal cells, PTEN and its downstream target PI3K maintain the dynamic balance of PIP2 and PIP3 by regulating their phosphorylation levels. When the expression of PTEN is reduced or absent, the dephosphorylation of PIP3 is limited, and it cannot be transformed into PIP2. The accumulation of PIP3 stimulates the activation of Akt, an important central link in the PTEN/PI3K/Akt signaling pathway, thereby stimulating the expression of downstream molecules [18]. Among these, P27 is a negative regulator of the cell cycle, and cyclin D1 is a key protein that regulates cell proliferation in the G1 phase. P27 binds to cyclin D1 and inhibits its activity, thus preventing cell cycle progression from G1 to S phase and thereby inhibiting cell proliferation [19]. Lv *et al* [20] found that miR-26a-5p was overexpressed in liver cancer, which caused a decrease in P27 expression and an increase in cyclin Dl expression, thus promoting cell cycle progression from the G1 to the S phase and promoting the proliferation of liver cancer cells. The PTEN/PI3K/Akt signaling pathway plays an important regulatory role in tumor cell cycle progression and arrest. In the present study, both the overexpression of GAS5 and the inhibition of miR-26a-5p could promote the expression of PTEN and thus reduce the levels of PI3K, p-Akt, and cyclin D1 downstream, while the expression level of P27 was increased. The expression of PTEN in the lncRNA GAS5 + miR-26a-5p group decreased, while the levels of PI3K, p-Akt, and cyclin D1 increased compared to in the GAS5 group, and the expression level of P27 decreased. This suggests that overexpression of GAS5 could regulate the expression of cyclin D1 and P27 by downregulating the expression of miR-26a-5p, thus activating the PTEN/PI3K/Akt signaling pathway, and arrest the cell cycle of HCC cells, which would inhibit proliferation and promote apoptosis.

In conclusion, GAS5 is expressed at low levels in HCC tissue, which may inhibit the activation of the PTEN/PI3K/Akt signaling pathway by upregulating the expression of miR-26a-5p, thereby affecting the expression of downstream cyclin D1 and regulating cancer cell proliferation and apoptosis.

Acknowledgments
Not applicable.

Funding
Not applicable.

Conflicts of interest
The authors indicated no potential conflicts of interest.

Author contributions
All authors contributed to data acquisition, data interpretation, and reviewed and approved the final version of this manuscript.

Data availability statement
Not applicable.

Ethical approval
Not applicable.

References

1. Zhao SN, Chen AX, Cao JY, et al. Neurotrophin 3 hinders the growth and metastasis of hepatocellular carcinoma cells. Oncol Transl Med. 2020;6(4):143-152.
2. Yang WS, Zeng XF, Liu ZN, et al. Diet and liver cancer risk: a narrative review of epidemiological evidence. Br J Nutr. 2020;124(3):330-340.
3. Kairaluoma V, Kemi N, Pohjanen VM, et al. Tumour budding and tumour-stroma ratio in hepatocellular carcinoma. Br J Cancer. 2020;123(1):38-45.
4. Cao S, Liu W, Li F, et al. Decreased expression of lncRNA GAS5 predicts a poor prognosis in cervical cancer. Int J Clin Exp Pathol. 2014;7(10):6776-6783.
5. Liu Y, Zhao J, Zhang W, et al. lncRNA GAS5 enhances G1 cell cycle arrest via binding to YBX1 to regulate p21 expression in stomach cancer. Sci Rep. 2015;5:10159.
6. Xue D, Zhou C, Lu H, et al. LncRNA GAS5 inhibits proliferation and progression of prostate cancer by targeting miR-103 through AKT/mTOR signaling pathway. Tumour Biol. 2016. doi: 10.1007/s13277-016-5429-8. Epub ahead of print.
7. Zhu WJ, Yan Y, Zhang JW, et al. Effect and mechanism of miR-26a-5p on proliferation and apoptosis of hepatocellular carcinoma cells. Cancer Manag Res. 2020;12:3013-3022.
8. Zhou Y, Xue R, Wang J, et al. Puerarin inhibits hepatocellular carcinoma invasion and metastasis through miR-21-mediated PTEN/AKT signaling to suppress the epithelial-mesenchymal transition. Braz J Med Biol Res. 2020;53(4):e8882.
9. Zhang F, Yang C, Xing Z, et al. LncRNA GAS5-mediated miR-1323 promotes tumor progression by targeting TP53INP1 in hepatocellular carcinoma. Onco Targets Ther. 2019;12:4013-4023.
10. Wang J, Zhu Y, Ni S, et al. LncRNA GAS5 suppressed proliferation and promoted apoptosis in laryngeal squamous cell carcinoma by targeting MiR-26a-5p and modifying ULK2. Cancer Manag Res. 2021;13:871-887.
11. Liu P, Cai S, Li N. Circular RNA-hsa-circ-0000670 promotes gastric cancer progression through the microRNA-384/SIX4 axis. Exp Cell Res. 2020;394(2):112141.
12. Liu Y, Yin L, Chen C, et al. Long non-coding RNA GAS5 inhibits migration and invasion in gastric cancer via interacting with p53 protein. Dig Liver Dis. 2020;52(3):331-338.
13. Song J, Shu H, Zhang L, et al. Long noncoding RNA GAS5 inhibits angiogenesis and metastasis of colorectal cancer through the Wnt/β-catenin signaling pathway. J Cell Biochem. 2019. doi: 10.1002/jcb.27743. Epub ahead of print.
14. Ma C, Wang W, Li P. LncRNA GAS5 overexpression downregulates IL-18 and induces the apoptosis of fibroblast-like synoviocytes. Clin Rheumatol. 2019;38(11):3275-3280.
15. Mihanfar A, Fattahi A, Nejabati HR. MicroRNA-mediated drug resistance in ovarian cancer. J Cell Physiol. 2019;234(4):3180-3191.
16. Zhang Z, Liang L, Cao G. Critical role of miR-26a-5p/Wnt5a signaling

in gambogic acid-induced inhibition of gastric cancer. J Biochem Mol Toxicol. 2021;35(4):e22721.
17. Liu Y, Yang EJ, Shi C, et al. Histone Acetyltransferase (HAT) P300/CBP inhibitors induce synthetic lethality in PTEN-deficient colorectal cancer cells through destabilizing AKT. Int J Biol Sci. 2020;16(11):1774-1784.
18. Chatterjee N, Pazarentzos E, Mayekar MK, et al. Synthetic essentiality of metabolic regulator PDHK1 in PTEN-deficient cells and cancers. Cell Rep. 2019;28(9):2317-2330.e8.
19. Yin G, Zhang B, Li J. miR-221-3p promotes the cell growth of non-small cell lung cancer by targeting p27. Mol Med Rep. 2019;20(1):604-612.
20. Lv P, Qiu X, Gu Y, et al. Long non-coding RNA SNHG6 enhances cell proliferation, migration and invasion by regulating miR-26a-5p/MAPK6 in breast cancer. Biomed Pharmacother. 2019;110:294-301.

DOI 10.1007/s10330-021-0507-7
Cite this article as: Yi ZL, Guo XG, Jiang XX, et al. Effects of long non-coding RNA GAS5 on proliferation and apoptosis of hepatocellular carcinoma cells through miR-26a-5p action. Oncol Transl Med. 2022;8(3):126–134.

Oncology and Translational Medicine
DOI 10.1007/s10330-021-0516-6

June 2022, Vol. 8, No. 3, P135–P139

ORIGINAL ARTICLE

Prognostic value of serum carcinoembryonic antigen combined with nutritional status control score in patients with colorectal cancer*

Yichao Zhang (✉), Biao Wang, Yongchuan Zhang, Gang Xiong, Xiao Pang

Department of Gastroenterology, Dazhou Central Hospital, Dazhou 635000, China

Abstract

Objective To investigate the prognostic value of serum carcinoembryonic antigen (CEA) and controlling nutritional status (CONUT) score in patients with colorectal cancer.

Methods We retrospectively studied 261 patients with colorectal cancer in our hospital. The patients were divided into two groups by CONUT = 3 and CEA = 5 ng/mL, and the effects of CONUT score and CEA level on the prognosis and clinicopathological parameters were statistically analyzed.

Results (1) Different CONUT scores were significantly correlated with age, tumor diameter, differentiation type, and T stage ($P < 0.05$). The older the patient was, the larger the tumor diameter, undifferentiated tumor, and T stage were, the higher the CONUT score was. (2) Seventy-five patients died during the follow-up period, and 45 patients died of progression or recurrence of colorectal cancer. The 5-year overall survival (OS) rate of the low CONUT score group was significantly higher than that of the high CONUT score group, and the 5-year OS rate of the low CEA group was significantly higher than that of the high CEA group; the difference was statistically significant ($P < 0.01$). (3) According to the serum CEA level and CONUT score, the 5-year survival rates of $CEA^{low}/CONUT^{low}$, $CEA^{low}/CONUT^{high}$, $CEA^{high}/CONUT^{low}$, and $CEA^{high}/CONUT^{high}$ were 84.7%, 69%, 55.3%, and 36.1% respectively, with statistical significance ($P <0.01$). (4) The Cox multivariate analysis showed that age, CONUT score, CEA combined with CONUT score, lymph node metastasis, and distant metastasis were independent risk factors for the prognosis of colorectal cancer patients.

Conclusion: The combination of CEA detection and CONUT score can more accurately judge the prognosis of colorectal cancer patients.

Received: 3 September 2021
Revised: 10 November 2021
Accepted: 21 December 2021

Key words: colorectal cancer; carcinoembryonic antigen; nutritional status control score

Cancer resection combined with regional lymph node dissection is the main treatment for colorectal cancer, but several patients relapse after complete tumor resection (R0 resection) [1]. The latest progress in chemotherapy has improved the prognosis of unresectable patients, and early detection of recurrence can effectively improve the survival rate of patients [2]. Serum tumor markers (TMS) are easy to measure and have potential practical value for diagnosis, predicting survival, and monitoring postoperative recurrence [3]. Carcinoembryonic antigen (CEA) and carbohydrate antigen (CA) 19-9 are the most commonly used tumor markers for diagnosing, monitoring, and predicting the prognosis of patients with colorectal cancer [4]. Recent studies have shown that the prognosis of various types of cancer is also affected by the patient's inflammatory state, immune function, and nutrition, among which the correlation between nutritional status and cancer prognosis is particularly significant [5]. Controlling nutritional status (CONUT) score, including serum albumin, total cholesterol, and peripheral lymphocyte count, is considered a new tool for assessing nutritional status [6]. The purpose of this study was to explore whether the combined application of TMS and CONUT score can more accurately reflect the prognosis of patients with CRC.

✉ Correspondence to: Yichao Zhang. Email: lanshuqinghwyy@163.com
* Supported by a grant from the Support Program of Sichuan Science and Technology Department (No. 2018sz2311).

Materials and method

Research objective

This was a retrospective study, wherein a total of 261 patients with stage I-IV colorectal cancer who underwent colorectal resection between January 2007 and December 2015 were selected as the research subjects. The inclusion criteria were as follows: (1) This should be the first diagnosis and surgical treatment. (2) All cases were confirmed through surgery and pathology. (3) Clinical and follow-up data were complete. Clinicopathological results were evaluated according to the Japanese classification criteria for colorectal cancer, 8th edition. Patients were regularly examined for early recurrence through diagnostic imaging, including chest radiography, colonoscopy, ultrasound, and computed tomography. The first hematological examination after admission was taken as the baseline data, including serum albumin, total cholesterol, and peripheral blood lymphocyte count in the patient's records.

CONUT score

The CONUT score was calculated according to the patient's serum albumin, total cholesterol, and peripheral blood lymphocyte count. The specific criteria are presented in Table 1. These factors were scored according to the critical value, and the sum of these factors was regarded as the CONUT score. According to the CONUT score, the patients were divided into four groups: normal (score 0–1), mild malnutrition (score 2–4), moderate malnutrition (score 5–8), and severe malnutrition (score 9–12).

Statistical analysis

SPSS 20.0 and GraphPad Prism software (version 5.0) were used for data processing. The counting data were expressed as the number of cases, and the measurement data were expressed as the mean ± standard deviation. One-way ANOVA or chi-squared tests were used for comparison between groups. Kaplan-Meier analysis was used for survival evaluation, and the log-rank test was used for inter-group comparisons. The receiver operating characteristic (ROC) curve was used to determine the area under the curve (AUC) and the best cutoff value of the CONUT score. The Cox proportional hazards model was used to analyze prognostic factors that may affect overall survival (OS).

Table 1 CONUT scoring criteria

Index	Nutritional status			
	Normal (0–1)	Mild (2–4)	Moderate (5–8)	Severe (9–12)
Albumin (g/dL)	3.5–4.5 (0)	3.0–3.5 (2)	2.5–2.9 (4)	< 2.5 (6)
Total cholesterol (mg/dL)	> 180 (0)	140–180 (1)	100–139 (2)	< 100 (3)
Leukomonocyte (/mL)	> 1600 (0)	1200–1599 (1)	800–1199 (2)	< 800 (3)

Results

Relationship between CONUT score and clinicopathological features of patients

There were 140 patients, 79 patients, 38 patients, and 4 patients with normal, mild, moderate, and severe CONUT scores, respectively. According to the ROC analysis, the best cutoff value for OS was 3 points (AUC = 0.627, $P < 0.01$). According to these results, the patients were divided into two groups: high CONUT score group (CONUT score ≥ 3, $n = 79$) and low CONUT score group (CONUT score < 3, $n = 182$). The chi-squared test showed that the different CONUT scores were significantly correlated with patient age, tumor diameter, differentiation type, and T stage ($P < 0.05$). The older the patient was, the larger the tumor diameter, undifferentiated tumor, and T stage were, the higher the CONUT score was (Table 2).

Table 2 Relationship between CONUT scores and clinicopathological features

Index	High CONUT score ($n = 79$)	Low CONUT score ($n = 182$)	χ^2	P
Age (years)			5.381	0.020
< 70	38	60		
≥ 70	41	122		
Gender			0.144	0.704
Male	48	106		
Female	31	76		
Tumor diameter (cm)			0.033	0.856
< 4	53	120		
≥ 4	26	62		
Tumor location			3.162	0.075
Colon	50	135		
Rectum	29	47		
Differentiation type			11.580	0.001
Differentiated	64	172		
Undifferentiated	15	10		
T stage			9.189	0.002
T1/2	16	72		
T3/4	63	110		
Lymphatic metastasis			0.395	0.530
No	51	110		
Yes	28	72		
Vascular metastasis			1.049	0.306
No	58	122		
Yes	21	60		

Comparison of survival rates of patients in different CONUT score groups

Seventy-five patients died during the follow-up period, 45 died of colorectal cancer progression or recurrence, and 30 died of other causes, including other cancers (n = 12), pneumonia (n = 6), stroke (n = 5), myocardial infarction (n = 4), and other unknown causes (n = 3). There were no surgery-related deaths. The 5-year OS rate (75.8%, 138/182) in the low CONUT score group was significantly higher than that in the high CONUT score group (54.4%, 43/79) (P < 0.01; Fig. 1).

Comparison of survival rate of patients with different serum CEA levels

Serum CEA levels ranged from 0.1 to 1166 ng/mL, with an average of 16.2 ng/ml. According to the serum CEA concentration, the patients were divided into high CEA (≥ 5 ng/mL, n = 89) and low CEA groups (< 5 ng/mL, n = 172). The 5-year OS rate of patients with low CEA levels (82.6%, 142/172) was significantly higher than that of patients with high CEA levels (43.8%, 39/89) (P < 0.01; Fig. 2).

Serum CEA combined with CONUT score to evaluate the prognosis of patients

Based on the serum CEA level and the CONUT score, the patients were divided into four groups: CEA^{low}/con ut^{low} (n = 128), CEA^{low}/$CONUT^{high}$ (n = 44), CEA^{high}/$CONUT^{low}$ (n = 53), and CEA^{high}/$CONUT^{high}$ (n = 36). According to the ROC curve, the AUC values of CEA level, CONUT score, and combined detection in predicting the prognosis of patients with colorectal cancer were 0.66 (P < 0.01), 0.627 (P < 0.01) and 0.71 (P < 0.0001), respectively, suggesting that combined detection is more valuable in predicting OS in patients with colorectal cancer, as shown in Table 3. The 5-year OS rates of the cealow/contlow, cealow/conthigh, ceahigh/contlow, and ceahigh/thigh were 84.7%, 69%, 55.3%, and 36.1%, respectively. The difference was statistically significant (P < 0.01), as shown in Fig. 3.

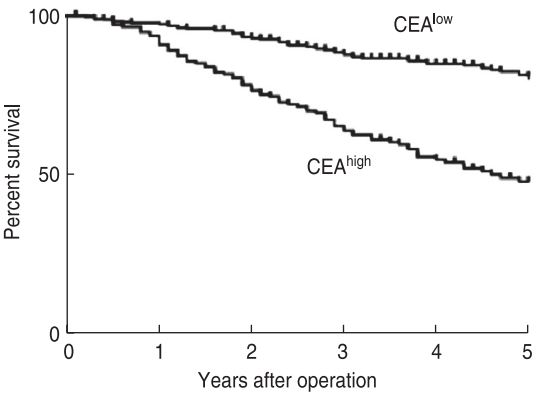

Fig. 2 Comparison of survival of patients with different serum CEA levels

Multivariate analysis of patients' survival rate

The Cox multivariate analysis showed that age, CONUT score, t-CONUT score, lymph node metastasis, and distant metastasis were independent risk factors affecting the prognosis of patients with colorectal cancer. Data was shown in Table 4.

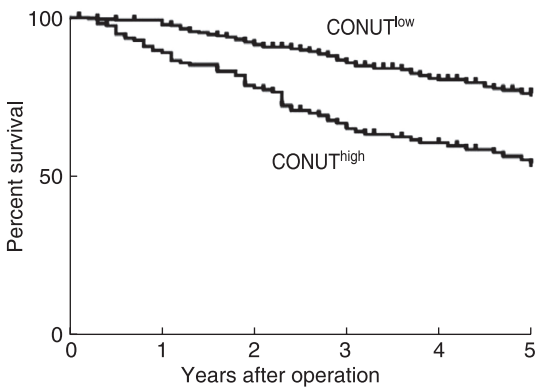

Fig. 1 Comparison of survival of patients in different CONUT scoring groups

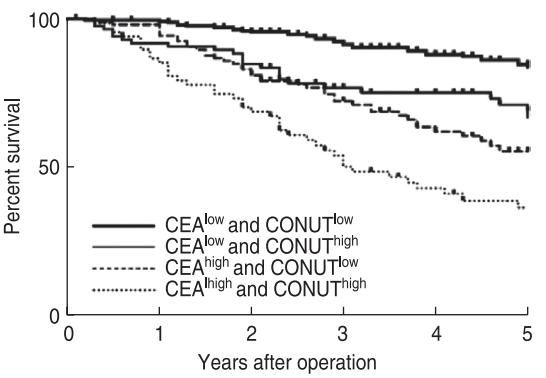

Fig. 3 Comparison of survival of patients with different serum CEA and CONUT scores

Table 3 Patient outcomes judged by three methods

Index	Sensitivity (%)	Specificity (%)	False positive (%)	False negative (%)	Positive predictive (%)	Negative predictive (%)
CEA	86.33	62.60	38.50	14.67	97.00	15.50
CONUT	92.00	76.00	26.00	8.00	98.50	33.33
Joint detection	97.50	63.50	38.50	2.50	97.88	42.64

Table 4 Multivariate analysis affecting patient survival

Index	β	SE	Wald	df	*P*	95%CI
Age	0.363	0.541	0.985	1	0.341	0.652–2.632
Gender	0.287	0.369	0.254	1	0.896	0.142–1.874
CEA	0.869	0.326	7.133	1	0.059	1.261–4.502
CONUT	0.678	0.335	4.078	1	0.041	1.021–3.980
T-Conut	0.189	0.268	8.464	1	0.009	0.495–1.398
lymphatic metastasis	0.523	0.296	2.181	1	0.038	0.951–2.993
Transfer far away	0.452	0.166	2.632	1	0.030	0.864–3.336
Degrees of differentiation	0.240	0.263	0.830	1	0.369	0.472–1.318
Tumor diameter	0.359	0.523	0.512	1	0.636	0.538–3.815

Discussion

The results of this study show that the CONUT score has a certain reference value in predicting the prognosis of patients with colorectal cancer, which is similar to that of previous reports, and proves the significance of CONUT score in postoperative patients with several cancers [7]. Previous studies have also shown that the CONUT score is an effective prognostic indicator for patients with metastatic colorectal cancer receiving first-line chemotherapy [8]. Conut scores included serum albumin, total cholesterol, and peripheral blood lymphocytes. Albumin, the most abundant plasma protein, is produced in the liver and accounts for a large proportion of all plasma proteins. It is a standard factor for evaluating the nutritional status of patients. It has been reported that [9] serum albumin is closely related to the prognosis of various cancers, including colon cancer. Peripheral blood lymphocytes are also considered to reflect the nutritional status and immune function of patients [10]. Lymphocytes include CD4 + and CD8 + T cells, natural killer cells, γ-δ T cells, and B cells, whose functions are closely related to tumor immunity. Therefore, the decrease in the number of these cells may be related to the impairment of tumor immune function, resulting in tumor progression. Some studies have shown that the number of tumor-infiltrating lymphocytes is related to the prognosis of cancer [11]. In addition, the decrease in the number of immune cells in the peripheral blood and cancer tissues is related to the poor prognosis of various cancers. Therefore, peripheral blood lymphocytes may be a good index to reflect the state of cellular immunity, including acquired immunity and humoral immunity.

The prognostic nutritional index (PNI), which includes serum albumin level and peripheral blood lymphocytes, is one of the most commonly used indicators to evaluate nutritional status [12]. Recently, PNI was found to be closely related to the prognosis of various types of cancer, indicating that nutritional status and immune status are prognostic indicators of cancer patients. In addition to serum albumin and peripheral blood lymphocytes, the OUT score also includes the measurement of serum cholesterol. It has been reported that [13] serum cholesterol is related to tumor progression and patient survival in various cancers, including colorectal cancer. This study also proved that serum CEA levels are closely related to the prognosis of patients with colorectal cancer. However, it should be noted that the CONUT score is effective in predicting the prognosis of patients with colorectal cancer, regardless of the serum CEA level. Serum CEA mainly reflects the tumor status, while the CONUT score primarily reflects the overall status of patients, including their nutritional status and immune status. According to the ROC analysis of this study, the combination of these two factors (t-cont) may provide more accurate prognostic information for patients with colorectal cancer than any factor alone. Considering the indications for adjuvant chemotherapy, the combined detection of the two may be helpful in clinical practice.

Migita *et al.* [14] used PNI to assess the preoperative immunonutritional status of patients and found that a low PNI score was associated with a higher risk of non-cancer death. A similar study showed that [15], compared with patients with high PNI scores, elderly patients with gastric cancer with a low PNI score had an increased risk of respiratory failure due to pneumonia. Overall, these findings suggest that poor nutritional status increases the risk of dying from non-cancer-related diseases after surgery. This suggests that it is beneficial to use patient-related factors to predict the prognosis of cancer patients.

In conclusion, this study found that t-CONUT is an effective index for evaluating the prognosis of patients with colorectal cancer. In view of the rapid, simple, and noninvasive determination of serum markers, t-CONUT may be a useful biomarker in a routine clinical setting. However, this study also has some limitations: (1) This study is a retrospective study; therefore, it is easy to produce a certain offset. (2) In this study, patients were divided into high and low groups with a cutoff value of 3. However, the cutoff values reported in different

reports are different, and the best cutoff value has not been recognized. (3) This was a single-center study. The number of patients included in the study was effective. A larger-scale, prospective, randomized, and controlled trial is needed to confirm this result.

Acknowledgments

Not applicable.

Funding

This study was supported by a grant from the Support Program of Sichuan Science and Technology Department (No. 2018sz2311).

Conflicts of interest

The authors indicated no potential conflicts of interest.

Author contributions

Yichao Zhang and Biao Wang contributed conception and design of the study. Yichao Zhang and Yongchuan Zhang drafted the manuscript. Gang Xiong and Xiao Pang examined research indicators and assisted in data collection. All authors read, discussed and approved the final manuscript.

Data availability statement

The data that support the findings of this study were available from the corresponding author upon reasonable request.

Ethical approval

Not applicable.

References

1. Bullman S, Pedamallu CS, Sicinska E, et al. Analysis of Fusobacterium persistence and antibiotic response in colorectal cancer. Science. 2017;358(6369):1443-1448.
2. Rex DK, Boland CR, Dominitz JA, et al. Colorectal cancer screening: recommendations for physicians and patients from the U.S. multi-society task force on colorectal cancer. Gastroenterology. 2017;153(1):307-323.
3. Ganesh K, Stadler ZK, Cercek A, et al. Immunotherapy in colorectal cancer: rationale, challenges and potential. Nat Rev Gastroenterol Hepatol. 2019;16(6):361-375.
4. Keum N, Giovannucci E. Global burden of colorectal cancer: emerging trends, risk factors and prevention strategies. Nat Rev Gastroenterol Hepatol. 2019;16(12):713-732.
5. Ho CL, Tan HQ, Chua KJ, et al. Engineered commensal microbes for diet-mediated colorectal-cancer chemoprevention. Nat Biomed Eng. 2018;2(1):27-37.
6. Kuroda D, Sawayama H, Kurashige J, et al. Controlling Nutritional Status (CONUT) score is a prognostic marker for gastric cancer patients after curative resection. Gastric Cancer. 2018;21(2):204-212.
7. Ryo S, Kanda M, Ito S, et al. The controlling nutritional status score serves as a predictor of short- and long-term outcomes for patients with stage 2 or 3 gastric cancer: analysis of a multi-institutional data set. Ann Surg Oncol. 2019;26(2):456-464.
8. Sun X, Luo L, Zhao X, et al. Controlling Nutritional Status (CONUT) score as a predictor of all-cause mortality in elderly hypertensive patients: a prospective follow-up study. BMJ Open. 2017;7(9):e015649.
9. Ahiko Y, Shida D, Horie T, et al. Controlling nutritional status (CONUT) score as a preoperative risk assessment index for older patients with colorectal cancer. BMC Cancer. 2019 Nov 6;19(1):946.
10. Wada H, Dohi T, Miyauchi K, et al. Prognostic impact of nutritional status assessed by the Controlling Nutritional Status score in patients with stable coronary artery disease undergoing percutaneous coronary intervention. Clin Res Cardiol. 2017;106(11):875-883.
11. Takagi K, Yagi T, Umeda Y, et al. Preoperative Controlling Nutritional Status (CONUT) score for assessment of prognosis following hepatectomy for hepatocellular carcinoma. World J Surg. 2017;41(9):2353-2360.
12. Yoshida N, Baba Y, Shigaki H, et al. Preoperative Nutritional Assessment by Controlling Nutritional Status (CONUT) is useful to estimate postoperative morbidity after esophagectomy for esophageal cancer. World J Surg. 2016;40(8):1910-1917.
13. Takagi K, Umeda Y, Yoshida R, et al. Preoperative controlling nutritional status score predicts mortality after hepatectomy for hepatocellular carcinoma. Dig Surg. 2019;36(3):226-232.
14. Migita K, Takayama T, Saeki K, et al. The prognostic nutritional index predicts long-term outcomes of gastric cancer patients independent of tumor stage. Ann Surg Oncol. 2013;20(8):2647-2654.
15. Watanabe M, Iwatsuki M, Iwagami S, et al. Prognostic nutritional index predicts outcomes of gastrectomy in the elderly. World J Surg. 2012;36(7):1632-1639.

DOI 10.1007/s10330-021-0516-6
Cite this article as: Zhang YC, Wang B, Zhang YC, et al. Prognostic value of serum carcinoembryonic antigen combined with nutritional status control score in patients with colorectal cancer. Oncol Transl Med. 2022;8(3):135–139.

Oncology and Translational Medicine
DOI 10.1007/s10330-021-0513-3

June 2022, Vol. 8, No. 3, P140–P145

ORIGINAL ARTICLE

The role of OR51E2 in colon cancer and rectal adenocarcinoma and the potential underlying mechanism

Shujia Chen[1], Siang Wei[2], Jiwei Wang[3] (✉)

[1] Department of Gastroenterology, Panjin Central Hospital Affiliated to Jinzhou Medical University, Panjin 124000, China
[2] Shanghai Institute of Cardiovascular Diseases, Zhongshan Hospital, Fudan University, Shanghai 200032, China
[3] Department of Gastrointestinal Surgery, Xuzhou Central Hospital, Xuzhou 221009, China

Abstract

Objective Short-chain fatty acids (SCFAs) produced by intestinal microbiota influence the pathogenesis and development of several intestinal diseases. OR51E2 is a newly discovered SCFA receptor. At present, research on the link between OR51E2 and intestinal cancer is limited. This study aimed to analyze the relationship between OR51E2 and colorectal cancer.

Methods Bioinformatic analysis revealed the OR51E2 protein expression pattern in different parts of the intestine, regulation of related proteins, and immune cell infiltration. The expression pattern and prognostic value of OR51E2 in colon and rectal cancer was determined, and the miRNAs targeting OR51E2 were predicted.

Results The expression level of OR51E2 was relatively high in the colon, small intestine, and duodenum. In addition, OR51E2 expression level was significantly reduced in colon and rectal cancer. A positive correlation between OR51E2 and immune cells was observed, which was associated with the survival of patients with colon and rectal cancer (hazard ratio: 1.5). Further, miR-96-5p and miR-1271-5-p were predicted to target OR51E2.

Conclusion OR51E2 plays an important positive role in the survival of patients with colon cancer and rectal adenocarcinoma.

Received: 23 August 2021
Revised: 16 September 2021
Accepted: 25 October 2021

Key words: OR51E2; colon cancer; rectal cancer; targeted microRNA; protein-protein interaction

Short-chain fatty acids (SCFAs) are the main metabolites produced by specific colonic anaerobic bacteria after fermenting dietary fiber. They mainly include acetic, propionic, butyric, valeric, and caproic acid [1]. SCFAs diffuse through or are actively absorbed by colonic epithelial cells and then enter the blood circulation. On the one hand, most SCFAs can be metabolized to produce energy. On the other hand, they can be used to epigenetically regulate HDACi genes [2]. SCFAs regulate peripheral immunity and the immune response in the central nervous system (CNS). Decreased dietary fiber intake or restriction of the intestinal microbiota is related to the development of inflammatory bowel disease [3–6], emphasizing that SCFAs are important immunomodulatory metabolites. SCFAs function by binding to SCFA receptors. Most of the SCFA receptors discovered to date are G protein-coupled receptors (GPRs), including GPR41, GPR43, and GPR109. GPR41 and GPR43, which are also known as free fatty acid receptors 3 (FFAR3) and 2 (FFAR2), are widely present in various cell types, such as immune and intestinal epithelial endocrine cells. For example, GPR43 can be expressed in large amounts in enteroendocrine cells, immune cells, and adipocytes, while GPR41 is widely expressed in smooth muscle, enteroendocrine, and nerve cells, among others. GPR109A can be expressed in large intestinal epithelial cells, colon cells, and hepatocytes and is abundantly expressed in fat and immune cells.

✉ Correspondence to: Jiwei Wang. Email: zxyywv82847@126.com

GPR43 and GPR41 is activated by acetic, propionic, and butyric acid, and GPR109A is activated by butyric acid. By activating GPRs, SCFAs can activate the signal transduction pathway of the immune response and exert anti-inflammatory effects on the intestinal mucosa. Olfactory receptor 78 (Olfr78), also known as OR51E2, is a newly discovered SCFA receptor that is expressed in a variety of tissues [7]. The *OR51E2* gene is upregulated in prostate cancer [8]. Ligand-induced activation of *OR51E2* also affects the proliferation, differentiation, and melanogenesis of melanocytes [9]. *OR51E2* plays a pathophysiological role in blood pressure regulation, as well as in the development of melanoma and prostate tumors. As an SCFA receptor, *OR51E2* may help maintain the physiological function of the intestine in intestinal cancer; however, current research on the role of *OR51E2* in intestinal cancer remains limited. Therefore, an in-depth analysis of its practical significance in the intestine is needed.

Recent studies have shown the relationship between *OR51E2* and immune and blood pressure regulation [9–10], but there is little data on differential *OR51E2* expression and and its role in the physiology and pathology of intestinal cancer. This study aimed to analyze the pathological and clinical features of the SCFA receptor *OR51E2* in colon and rectal adenocarcinoma. It also aimed to predict *OR51E2*-targeting miRNAs using bioinformatics analysis and provide a scientific basis for the treatment and prevention of colon cancer.

Materials and methods

Differential OR51E2 expression in tissues

The expression levels of the SCFA receptors FFAR2, FFAR3, and *OR51E2* in the mouse intestine (large intestine, small intestine, colon, and duodenum) and heart tissue were obtained from the National Center for Biotechnology Information (NCBI) database (https://pubmed.ncbi.nlm.nih.gov/). The results are presented as heatmaps.

GO functional enrichment and network interaction analysis of OR51E2

UniProt database (https://www.uniprot.org/) was used to functionally reannotate OR51E2, and Gene MANIA software was used to analyze the protein–protein interactions involving OR51E2, coexpression, and the signaling pathway of related proteins.

OR51E2 and its correlation with immune cell infiltration in colon and rectal cancer

The Gene Expression Profiling Interactive Analysis (GEPIA) database (http://gepia.cancer-pku.cn/) was used to analyze OR51E2 gene expression and normal tissues in colon cancer and rectal adenocarcinoma, with statistical significance set at $P \leq 0.05$. The Tumor IMmune Estimation Resource (TIMER) database (http://cistrome.dfci.harvard.edu/TIMER/) was used to explore the correlation between *OR51E2* and different immune cells, namely B cells, CD4-T cells, CD8-T cells, neutrophils, macrophages, and dendritic cells. Pearson's correlation coefficient was used to express the correlation between *OR51E2* and immune cells.

Prognostic analyses of OR51E2 in colon cancer and rectal cancer

The online database Kaplan-Meier Plotter (http://www.kmplot.com/) was used to analyze the prognosis of breast cancer patients through receiver operating characteristic curves (ROC) for hub genes. The follow-up period was six months.

OR51E2 targeted by miRNAs and predicted regulatory mechanism

TargetScan 7.2 (http://www.targetscan.org/) software was used to predict the miRNAs targeting OR51E2 strongly and conservatively in vertebrates (human, rat, mouse, rabbit, and chicken). Using the Kyoto Encyclopedia of Genes and Genomes database (https://www.kegg.jp/), miRNAs were predicted that could target OR51E2 to regulate intestinal and intestine-related acute or chronic diseases.

Results

Differential expression in tissues

Proteins can perform specific biological functions only when they are expressed in tissues. To show that OR51E2 plays an important role in the intestine and heart, we screened the expression level data of the large and small intestine, colon, duodenum, and heart using tissue-specific gene expression data obtained from the NCBI database, in which tissue samples were taken from adult mice. The results are shown in Fig. 1. OR51E2 was expressed at relatively high levels in the heart and colon and at low levels in the large intestine, small intestine, and duodenum. This suggests that OR51E2 plays an important role in the function and stabilization of the gut-mandrel.

GO functional enrichment and protein interaction network analysis of OR51E2

Interactions of two or more proteins can achieve certain biological functions. We used STRING (https://www.string-db.org/) to analyze protein–protein interactions of OR51E2, and the results (Fig. 2a) showed that *OR51E2* interacted with RTP4, CNG1, REEP5, GNB1, RTP3, GNAL, REEP3, RTP2, REEP1, and RTP1. Using Gene MANIA to analyze the relationship between

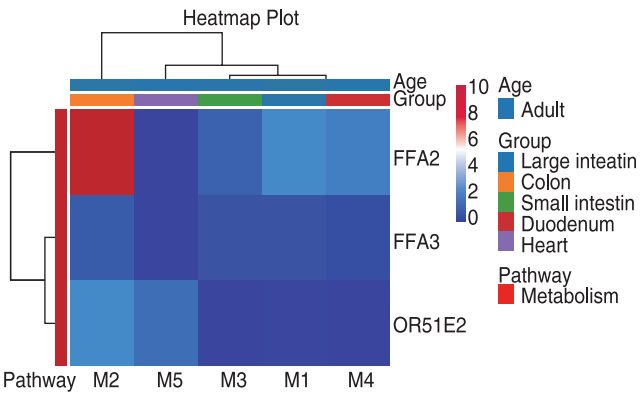

Fig. 1 Expression levels of SCFA receptors in the intestine and heart. Red and blue color scale indicates high and low expression levels, respectively

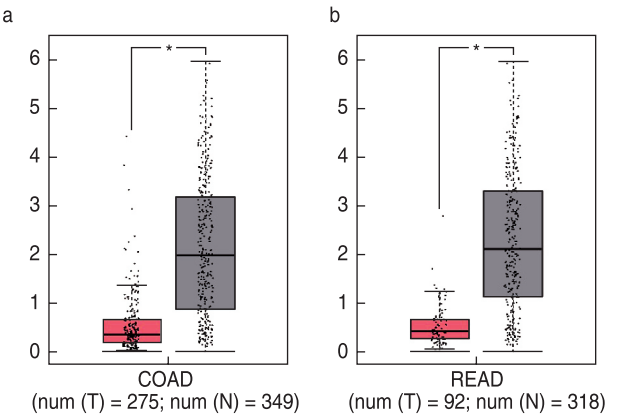

Fig. 3 OR51E2 expression level in intestinal cancer. Panel a shows *OR51E2* expression in 349 healthy people and 275 colon cancer patients. Panel b shows OR51E2 expression in 318 rectal cancer patients 92 healthy people. The red boxes represent cancer patients, and the gray boxes represent normal healthy people

OR51E2 and related proteins (Fig. 2b) and *Homo sapiens* as the data source, the coexpressed proteins were SEMG2, OR51E2, OR51E1, GNGT1, NRL, AKT3, KLK4, NKX3-1, KLK3, TGM4, SLC45A3, KLK2, NPY, PRAC1, ANO7, FAM159A, CPNE4, PAEP. Pathway: OR51E2, OR51E1, ARRB2, GNAL, GNB1, and GNGT1. By analyzing the relationship between OR51E2 and other proteins, it can provide an analytical basis for exploring the pathological mechanism of *OR51E2* in regulating intestinal cells.

Analysis of gene expression and immune cell infiltration in intestinal cancer

To understand whether *OR51E2* plays an important function in intestinal diseases, we analyzed the expression level of *OR51E2* in patients with colon or rectal cancer, including 275 patients with colon cancer with 349 corresponding controls and 318 patients with rectal cancer with 92 corresponding controls. OR51E2 expression level was significantly decreased in colon and rectal cancer ($P < 0.05$). In addition, stromal cell score and immune cell infiltration results can be used to study the immune infiltration between different samples. Through the differential expression of marker genes in different immune cells, the types and distribution of various immune cells in the sample can be analyzed, which can be used to study the differences in immune cell types in different cancers. Using the TIMER database, we analyzed the correlation between OR51E2 and different immune cells (B cells, CD4-T cells, CD8-T cells, dendritic cells, neutrophils, and macrophages). Pearson correlation coefficient was used to calculate the correlation between OR51E2 and different immune cells. Only four types

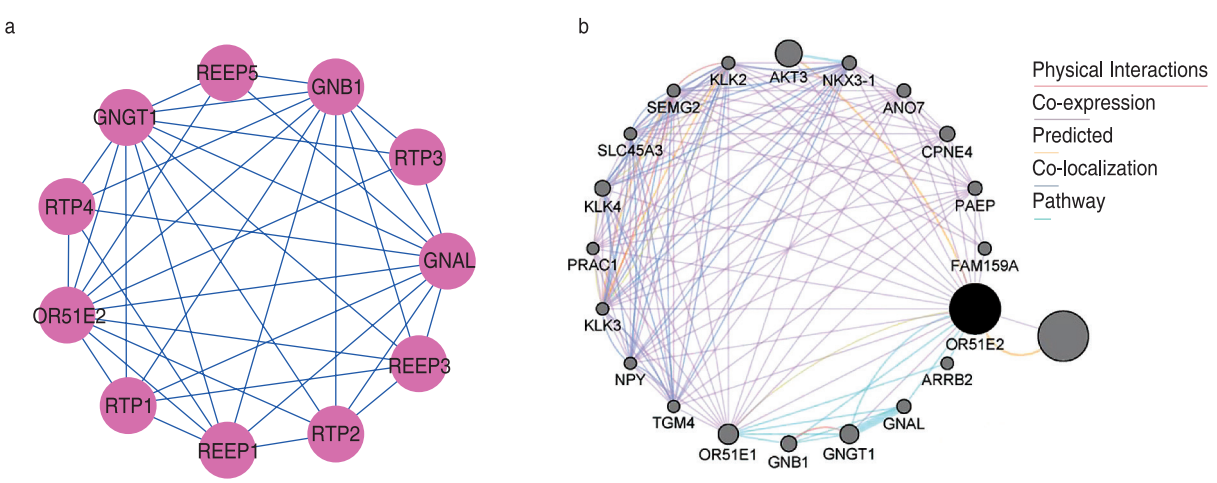

Fig. 2 Interactions between *OR51E2*-related proteins. Panel a shows the proteins interacting with *OR51E2*. Panel b shows the network diagram of *OR51E2*-related proteins mainly involving physical correlation, coexpression, prediction, colocalization, and signaling pathways

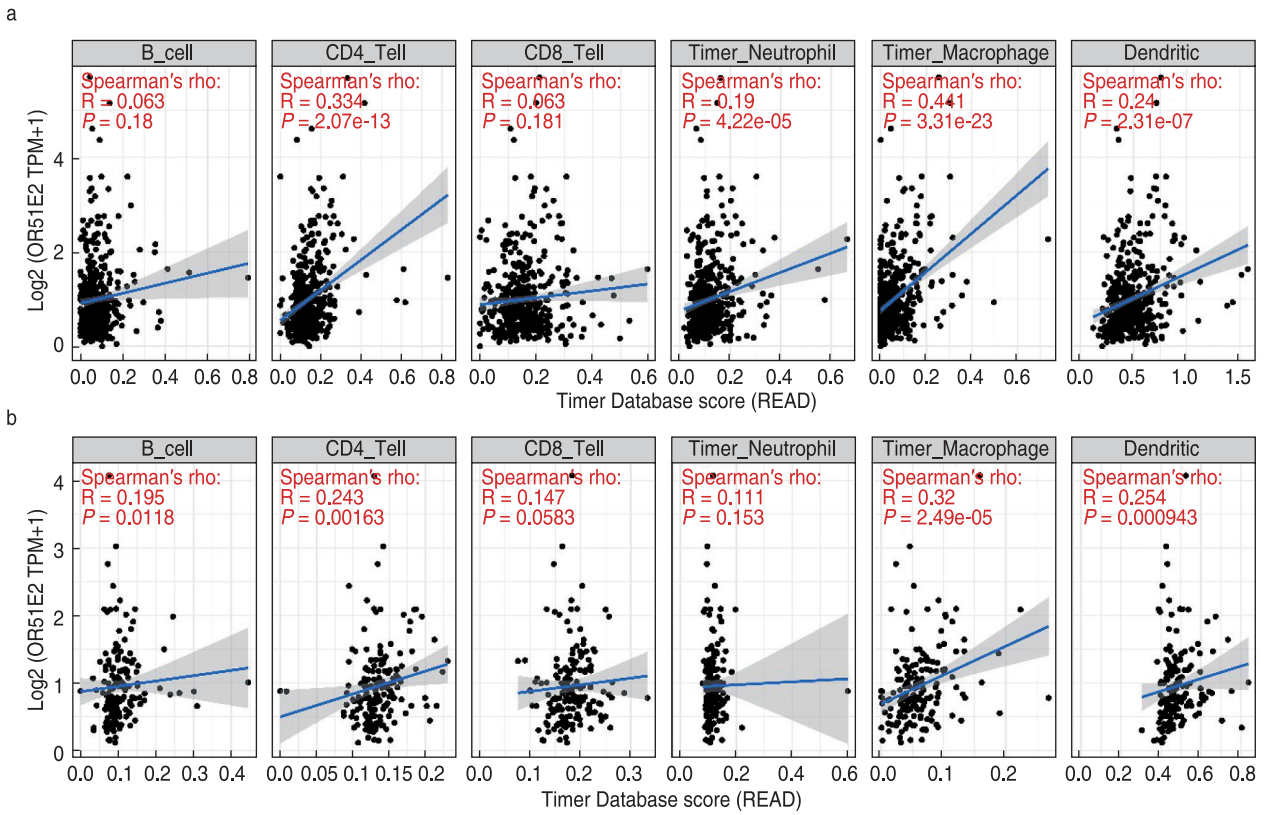

Fig. 4 Analysis of the survival status of *OR51E2* in intestinal cancer. Panel A shows the correlation of *OR51E2* with immune cells of colon cancer. Panel B shows the correlation of *OR51E2* with immune cells of rectal cancer. The R-value indicates the correlation, and statistical significance was set at $P < 0.05$

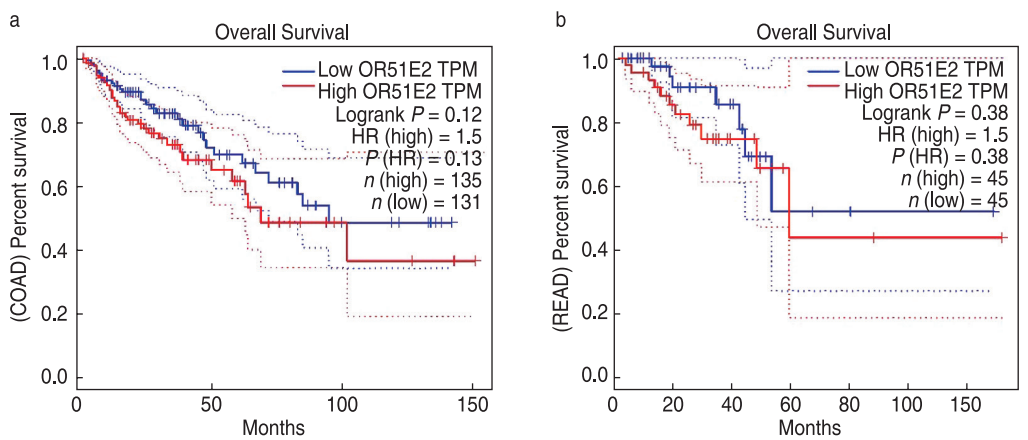

Fig. 5 Correlation between *OR51E2* and related immune cells in intestinal cancer. Panel a shows the survival analysis of *OR51E2* in colon cancer patients, of which 135 had high expression, and 131 had low expression. Panel b shows the survival analysis of *OR51E2* in rectal cancer patients, of which 45 had high expression levels and 45 had low expression levels. Blue represents the low expression group, and red represents the high expression group

of cells were found to be meaningful in colon cancer, namely CD4+ T cells (P = 2.07e-13), neutrophils (P = 4.22e-05), macrophages (P = 2.31e-23), and dendritic cells (P = 2.31e-07). Meanwhile, *OR51E2* gene expression level in rectal cancer was positively correlated with B cells (P = 0.0108), CD4+ T cells (P = 0.00168), macrophages (P = 2.49e-05), and dendritic cells (P = 0.000943).

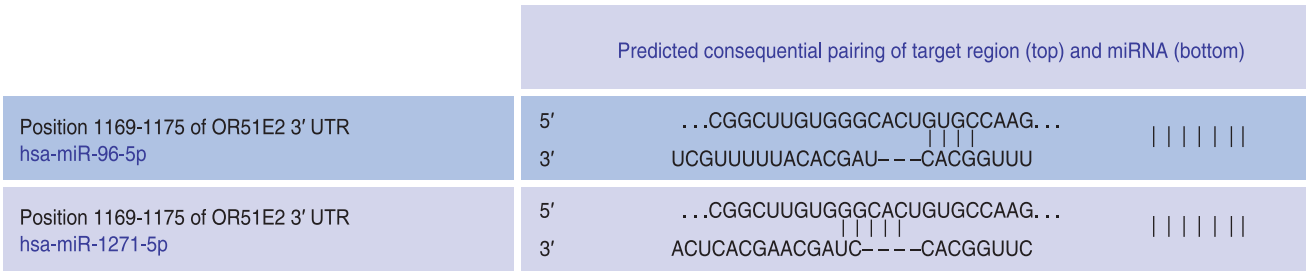

Fig. 6 Prediction of miRNAs targeting *OR51E2*

Survival curve analysis

Prognostic analysis showed that the *OR51E2* gene expression level was related to the survival duration of colon and rectal cancer patients. In Fig. 5a, 266 experimental patients were included, and the hazard ratio (HR) of colon cancer patients was 1.5 (log-rank P = 0.12, P [HR] = 0.13). In Fig. 5b, 90 experimental patients were included, and the HR of rectal cancer patients was 1.5 (log-rank P = 0.38, P [HR] = 0.38).

miRNA prediction

TargetScan 7.2 was used to predict the biological targets of miRNAs by searching for conserved 8mer, 7mer, and 6mer sites matching the seed region of each miRNA, and the reliability of the prediction results had high practicality [11]. TargetScan 7.2 predicted two miRNAs that were conserved in vertebrates, namely miR-96-5P and miR-1271-5-p (Fig. 6).

Discussion

The expression level of OR51E2 is related to the regulation of colitis and related cancer genes [12]; however, the pathological characteristics and role of OR51E2 in colon and rectal cancer remain unclear. This study confirmed that OR51E2 was highly expressed in colon and rectal cancer and was related to the survival time of clinical intestinal cancer patients. Using biological screening methods, we found that miR-96-5p and miR-1271-5-p are key players in the regulation of the pathological processes of the body via the signaling pathway that affects *OR51E2*.

GO functional enrichment analysis showed that *OR51E2* mainly played molecular biological functions in the sense of smell, GPRs, steroid hormone receptors, and signal receptors. Activation of OR51E2 triggers the Ca^{2+} retinal pigment epithelial cell-dependent signaling pathway. The downstream signaling pathway of *OR51E2* involves the activation of adenylate cyclase, ERK1/2, and AKT, and it regulates the migration and proliferation of retinal pigment epithelial cells [13]. In addition, OR51E2 is significantly upregulated in prostate cancer, and coexpression with TMPRSS2 leads to the loss of smell in coronary pneumonia [14]. However, studies on protein-interacting molecules related to OR51E2 are lacking. Multiple protein-phase interaction molecules with OR51E2 screened in this study provide a better understanding of the physiological and pathological mechanisms involved in OR51E2.

As a unique source of various immunoglobulins, B cells are an indispensable part of humoral immunity [15]. The dysregulation of B cells led to changes in space, phenotype, and function, including autoimmune diseases, infections, and cancers [16]. The CD4/CD8 ratio at the tumor-host interface was significantly related to recurrence-free and overall survival and had important implications for clinical prognosis [17]. Neutrophils, macrophages, and dendritic cells played a role in increasing the production and elimination of cytokines and immune cells, and therefore had a profound impact on the morbidity and mortality of cancer patients [18]. Liu *et al.* determined that macrophage migration inhibitor (MIF) promotes the proliferation and invasion of colon cancer cells by promoting the combination of CD74 and STAT1 [19]. Changes in the numbers of immune cells reflect immune disorder. When immune function was inhibited, CD8+ increased while CD4+, the CD4+/CD8+ ratio, and the number of immune cells decreased. The results of this study showed that OR51E2 protein levels were low in patients with colon and rectal cancer, while B cells, CD4+ T cells, macrophages, and dendritic cells were positively correlated with OR51E2 in colon and rectal cancer. This indicates that the expression of OR51E2 in intestinal cancer led to the decline of the body's immune level, which was consistent with our immunoassay results.

SCFA receptor proteins may play important roles not only in the passage of olfactory signals, but also in diseases, such as enteritis [20], prostate cancer [21], and hypertension [22]. Dietary fiber helps maintain the intestinal microbial ecology, host physiology, and health [23]. The SCFAs produced by the intake of dietary fiber are essential for regulating the host's intestinal immune response, which is necessary for the survival of intestinal microbes and metabolites [24]. These findings indicate

that OR51E2 expression is essential for the stability of the intestinal immune system. However, whether this differential expression influences intestinal cancer was unclear. Our study confirmed that OR51E2 expression level was significantly reduced in colon and rectal cancer and this reduced level is a mortality risk factor in patients with colon and rectal cancer.

In summary, after analyzing clinical data, we determined that *OR51E2* may be an effective biomarker for the detection of colon and rectal cancer. OR51E2 protein expression in cancer patients also led to the reduced immune levels, which predicted that *OR51E2* targets and regulates miRNAs. The findings present a target for regulating intestinal cancer, providing a scientific basis for effective detection and treatment of colon and rectal cancer. Despite these findings, our research has some limitations. The role of *OR51E2* was analyzed using bioinformatic tools, but these results should be validated *in vitro* and in clinical samples.

Acknowledgments
Not applicable.

Funding
Not applicable.

Conflicts of interest
The authors indicated no potential conflicts of interest.

Author contributions
Not applicable.

Data availability statement
Not applicable.

Ethical approval
Not applicable.

References

1. Wenzel TJ, Gates EJ, Ranger AL, et al. Short-chain fatty acids (SCFAs) alone or in combination regulate select immune functions of microglia-like cells. Mol Cell Neurosci. 2020;105:111-116.
2. Ganapathy V, Thangaraju M, Prasad PD, et al. Transporters and receptors for short-chain fatty acids as the molecular link between colonic bacteria and the host. Curr opin pharmacol. 2013;13:869-874.
3. Katagiri R, Goto A, Sawada N, et al. Dietary fiber intake and total and cause-specific mortality: the Japan Public Health Center-based prospective study. Am J Clin Nutr. 2020;111:1027-1035.
4. Li MM, Zhou Y, Zuo L, et al. Dietary fiber regulates intestinal flora and suppresses liver and systemic inflammation to alleviate liver fibrosis in mice. Nutrition. 2021;81:121-129.
5. Swann OG, Kilpatrick M, Breslin M, et al. Dietary fiber and its associations with depression and inflammation. Nutr Rev. 2020;7: 394-411.
6. Vitale M, Masulli M, Rivellese AA, et al. Pasta consumption and connected dietary habits: associations with glucose control, adiposity measures, and cardiovascular risk factors in people with Type 2 Diabetes-TOSCA. It study. Nutrients. 2019;12:101-110.
7. Miyamoto J, Kasubuchi M, Nakajima A, et al. The role of short-chain fatty acid on blood pressure regulation. Curr Opin Nephrol Hy. 2016; 25:379-383.
8. Xu LL, Stackhouse BG, Florence K, et al. PSGR, a novel prostate-specific gene with homology to a G protein-coupled receptor, is overexpressed in prostate cancer. Cancer Res. 2000;60:6568-6572.
9. Gelis L, Jovancevic N, Veitinger S, et al. Functional characterization of the odorant receptor 51E2 in human melanocytes. J Biol Chem. 2016;291:177-186.
10. Corrêa-Oliveira R, Fachi JL, Vieira A, et al. Regulation of immune cell function by short-chain fatty acids. Clin Transl Immunol. 2016;5:99-107.
11. Agarwal V, Bell G W, Nam J-W, et al. Predicting effective microRNA target sites in mammalian mRNAs. eLife. 2015;4:109-119.
12. Kotlo K, Anbazhagan AN, Priyamvada S, et al. The olfactory G protein-coupled receptor (Olfr-78/OR51E2) modulates the intestinal response to colitis. Am J Physiol Cell Physiol. 2020;318:129-138.
13. Jovancevic N, Khalfaoui S, Weinrich M, et al. Odorant receptor 51E2 agonist β-ionone regulates RPE cell migration and proliferation. Front Physiol. 2017;8:129-139.
14. Kerslake R, Hall M, Randeva HS, et al. Co-expression of peripheral olfactory receptors with SARS-CoV-2 infection mediators: Potential implications beyond loss of smell as a COVID-19 symptom. Int J Mol Med. 2020;46:949-956.
15. McLean KC, Mandal M. It takes three receptors to raise a B cell. Trends Immunol. 2020;41:629-642.
16. Lamaison C, Tarte K. Impact of B cell/lymphoid stromal cell crosstalk in B-cell physiology and malignancy. Immunol lett. 2019;215:12-26.
17. Wang K, Shen T, Siegal GP, et al. The CD4/CD8 ratio of tumor-infiltrating lymphocytes at the tumor-host interface has prognostic value in triple-negative breast cancer. Hum Pathol. 2017;69:111-129.
18. Singbartl K, Formeck CL, Kellum JA. Kidney-Immune System Crosstalk in AKI. Semi Nephrol. 2019;39:96-106.
19. LiuF, Jianxin Z, Jianbin S, et al. Effects of MIF on proliferation, migration, and STAT1 pathway of colon cancer cells. Oncol Transl Med. 2020;6:121-125.
20. Rodriguez M, Siwko S, Liu M. Prostate-specific G-protein coupled receptor, an emerging biomarker regulating inflammation and prostate cancer invasion. Curr Mol Med. 2016;16:526-532.
21. Souza MF, Kuasne H, Barros-Filho MC, et al. Circulating mRNA signature as a marker for high-risk prostate cancer. Carcinogenesis. 2020;41:139-145.
22. RR M, Marques FZ. Diet-related gut microbial metabolites and sensing in hypertension. J Hum Hypertens. 2021;35:162-179.
23. Makki K, Deehan EC, Walter J, et al. The impact of dietary fiber on gut microbiota in host health and disease. Cell Host Microbe. 2018;23:705-715.
24. Danneskiold-Samsøe NB, Dias de Freitas Queiroz Barros H, Santos R, et al. Interplay between food and gut microbiota in health and disease. Food Res Int. 2019;115:132-145.

DOI 10.1007/s10330-021-0513-3
Cite this article as: Chen SJ, Wei SA, Wang JW. The role of OR51E2 in colon cancer and rectal adenocarcinoma and the potential underlying mechanism. Oncol Transl Med. 2022;8(3):140–145.

Oncology and Translational Medicine
DOI 10.1007/s10330-021-0533-3
June 2022, Vol. 8, No. 3, P146–P149

ORIGINAL ARTICLE

Ultrasonographic and clinicopathologic features of benign Brenner tumors of the ovary*

Shuyu Wang (✉), Xiaomei Zhou

Department of Ultrasound, Zigong First People's Hospital, Zigong 643099, China

Abstract

Objective The aim of this study was to summarize and analyze the ultrasonographic and clinicopathologic features of benign brenner tumors of the ovary.

Methods Forty-six patients with brenner tumors of the ovary were included, and the imaging and pathologic features of the tumors were analyzed.

Results Thirty-eight cases were unilateral, while eight cases were bilateral. The tumors were located only in the left ovary in 32 patients and in the right ovary in six patients. The median diameter of the tumors was 62 mm, and the diameter ranged from 15 to 270 mm. Vascular tumors were not observed. Most of the tumors (22/46) showed micro-perfusion, while 16 tumors showed no blood flow signal. Acoustic signal shadows after the cysts were observed in 26 tumors, accounting for 57% of all brenner tumors. Fourteen patients showed unilocular or multilocular tumors with no distinct characteristics on ultrasonography. Sixteen masses showed a multilocular solid structure, accompanied by calcification and a post-mass shadow; the solid structure showed mild-to-moderate vascularization on Doppler examination. Sixteen masses showed a pure solid structure, accompanied by calcification, resulting in an acoustic shadow behind the tumor; the solid structure showed mild-to-moderate vascularization on Doppler examination.

Conclusion Some ultrasonographic features, including calcification with shadow, poor blood circulation of solid components, and mass localization, are helpful in the diagnosis of benign brenner tumors.

Received: 11 November 2021
Revised: 10 December 2021
Accepted: 28 December 2021

Key words: brenner tumor; ovary; clinicopathologic features

Brenner tumors are a type of ovarian epithelial tumor first reported by Fritz *et al.* in 1907. They often occur in women aged 50–70 years [1]. Brenner tumors are benign transitional cell tumors of the ovary but have the potential for malignancy. They account for approximately 3% of all ovarian epithelial tumors [2]. Careful histologic examination should be performed in clinics to exclude small malignant tumors that may involve brenner tumors [3]. Benign brenner tumors lack specific clinical symptoms and are mostly detected incidentally during routine physical examination or ultrasonography. Borderline and malignant brenner tumors can manifest as abdominal pain, vaginal bleeding, urinary retention, and ascites [4] owing maladjustment of estrogen levels. Complete preoperative ultrasonography is important for differentiating between benign and malignant adnexal tumors and formulating further treatment plans. However, although the International Organization for Ovarian Tumor Analysis has formulated imaging standards for detecting ovarian cancer, the ultrasonographic features of brenner tumors overlap with those of typical ovarian cancer, causing serious difficulties in image interpretation [5]. Therefore, this study retrospectively analyzed and summarized the ultrasonographic and clinicopathologic features of histologically confirmed benign brenner tumors in our hospital to provide a basis for the ultrasonographic diagnosis of affected patients.

Materials and methods

Study subjects

Forty-six patients with brenner tumors of the ovary treated in our hospital between January 2002 and January 2021 were included in the study. The inclusion criteria were as follows: (1) abnormal ovarian ultrasonographic findings with or without elevated CA125 levels

✉ Correspondence to: Shuyu Wang. Email: taoyoujianghwyy@163.com
*Supported by a grant from the Medical Research Project of the Sichuan Medical Association (No. s19332).

and nonspecific abdominal symptoms; (2) ovarian abnormalities detected for the first time; (3) history of surgical treatment; and (4) benign brenner tumor diagnosed on postoperative histopathology. Baseline data, such as age at diagnosis, menopause, serum CA125 level, risk of malignancy index, clinical symptoms, and histologic findings, were collected from the electronic medical record system of our hospital. The average age of the 39 patients was 43.6±7.8 years, including 5 patients with lateral ovarian mucinous cystadenoma, four with hysteromyoma, four with ovarian serous cystadenoma, two with adenomyosis, and one with endometrial polyp. Only seven patients had elevated serum CA125 levels, and the median CA125 level was 19 IU/L.

Instruments and methods

Prior to the examination, the patients were asked to empty their bladder and take the lithotomy position. The Mairui DC_ Type 8 color Doppler ultrasound diagnostic instrument and transvaginal (5–8 MHz) and transabdominal probes (3.5–5 MHz) were used. The uterus, pelvic cavity, and bilateral attachments of the patients were carefully scanned through the vagina, and patients with large tumors were scanned repeatedly using a transabdominal probe. The scanning focused on the size, boundary, envelope, relationship with surrounding tissues, internal echo, and blood flow of the masses.

Results

Histologic examination

Microscopically, the tumors were composed of well-defined and uniform epithelial islands located in dense fibrous stroma. The epithelial cells had characteristic coffee bean-like nuclei with longitudinal grooves and a pale cytoplasm (Fig. 1).

Ultrasonographic examination

Thirty-eight (82.7%) tumors occurred in the unilateral ovary and eight in the bilateral ovaries. Brenner tumors were diagnosed simultaneously. Two patients had ascites; their serum CA125 level increased, and no pleural effusion was found. The tumors were located only in the left ovary in 32 patients and in the right ovary in six patients. The median diameter of the tumors was 62 mm, with the diameter ranging from 15 to 270 mm, and the diameter of the largest solid structure was 40 mm (range: 0–85 mm). Thirty-six tumors contained solid components (Fig. 2a and 2b), and only 14 (30%) tumors contained pure cystic components. The cystic fluid was anechoic in 28 patients (Fig. 2c) and hypoechoic in two patients. The Doppler color signal was between NO and moderate, and no rich vascular tumors were found. Acoustic signal shadows after the cysts were observed in 26 tumors (Fig. 2d).

Difference between the ultrasonographic and clinical diagnoses

The tumors in 14 patients were unilocular or multilocular without distinct characteristics on ultrasonography and were correctly diagnosed as benign masses. Sixteen masses showed a multilocular solid structure, accompanied by calcification and a post-mass shadow; the solid structure showed mild-to-moderate vascularization on Doppler examination. Sixteen masses showed a pure solid structure, accompanied by calcification resulting in an acoustic shadow behind the tumor; the solid structure showed mild-to-moderate vascularization on Doppler examination. At the first diagnosis, the doctors performing the ultrasonography misdiagnosed four cases of benign brenner tumors as malignant. The median diameter of the four brenner tumors was 96 mm, and the maximum diameter was 270 mm, which was generally greater than the median

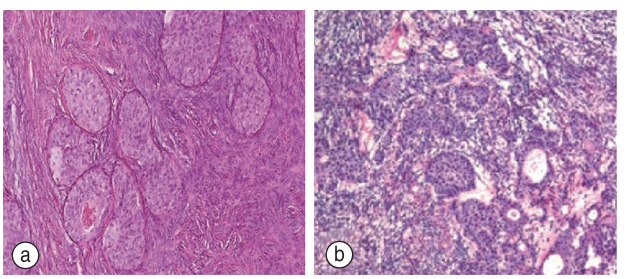

Fig. 1 Microscopic view of a benign Brenner tumor. (a) Large nuclei (HE staining × 200); (b) Interstitial fibrous hyperplasia of the tumor (HE staining × 400)

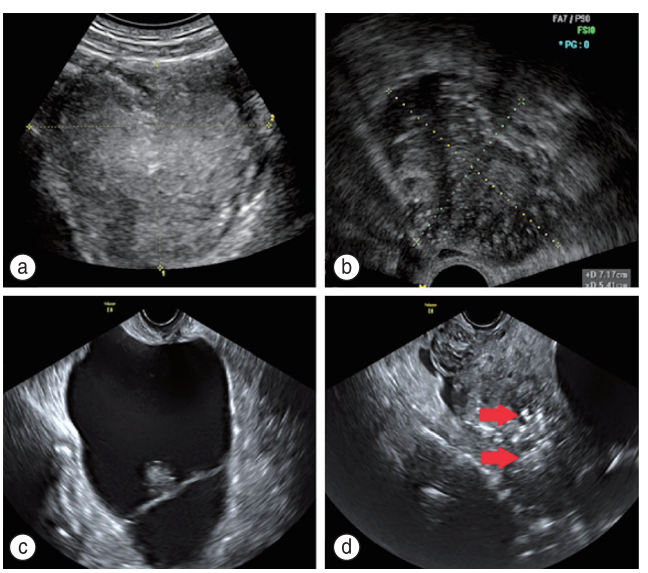

Fig. 2 Ultrasonographic features of a brenner tumor. (a, b) The tumor body contains solid components; (c) There is no echo in the cystic fluid of the tumor; (d) Post-cyst signal shadow

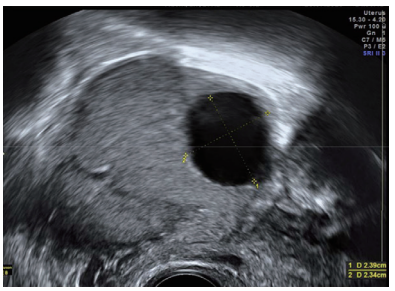

Fig. 3 Ultrasonographic image of a brenner tumor misdiagnosed as a malignant tumor

diameter of all tumors. Further, all four brenner tumors contained anechoic cystic components (Fig. 3).

Discussion

Brenner tumors usually occur in postmenopausal women, and most patients have no symptoms. Although the imbalance of estrogen activity can manifest as vaginal bleeding, only five patients in this study had abdominal pain or ascites, and the proportion of symptomatic patients was very low. Ovarian masses and elevated serum CA125 levels usually suggest malignant processes in postmenopausal women [6]. Studies have evaluated the correlation between the CA125 level and malignancy of ovarian tumors and found that the detection of tumor marker CA125 alone is not suitable for distinguishing between benign and malignant adnexal masses [7]. In this study, only two patients had elevated serum CA125 levels.

Dierickx *et al.* reported that experienced ultrasonography doctors failed to describe the unique ultrasonographic features of brenner tumors, and no other studies found unique images of brenner tumors [8]. Many benign brenner tumors show a complete solid structure on ultrasonography, while some may show cystic components, with or without a solid structure. In our study, color Doppler imaging showed poor vascularization of the solid components. In the literature, the calcification rate of brenner tumors based on ultrasonographic findings is approximately 50%. Researchers have found calcification in 15 patients with benign brenner tumors and 13 other patients on ultrasonography [9]. In this study, 32 brenner tumors containing solid components showed a sound shadow caused by calcification. Therefore, we conclude that the multiple calcifications observed on ultrasonography may be a key feature in the diagnosis of brenner tumors.

The laterality of brenner tumors varies greatly in different studies [10]. In this study, 82% of the brenner tumors occurred on the left side of the ovary. This is consistent with the findings reported by Dierickx *et al.*, indicating that brenner tumors are more common in the left ovary than in the right ovary. Only 18% of the brenner tumors in this study were bilateral; this rate is slightly higher than the range reported in the literature (5–14%) [11]. Brenner tumors are often associated with the risk of a second ovarian tumor. It has been reported that 30% of brenner tumors can be accompanied by other ovarian tumors. In this study, there were 13 patients with benign tumors, 5 patients with lateral ovarian mucinous cystadenoma, 4 patients with hysteromyoma, and 4 patients with ovarian serous cystadenoma. The sonogram of a brenner tumor can show a cystic, cystic solid, or solid mass. The cystic part can be separated, and blood flow signals can be detected during separation. The solid part is mostly hypoechoic, and the hypoechoic part is mostly accompanied by a strong echo formed by uncertain calcification, followed by attenuation. Brenner tumors have a certain misdiagnosis rate in most literature reports, which shows that it is difficult to distinguish between benign and malignant simple ovarian tumors on ultrasonography [12].

The varying ultrasonographic features and low incidence of brenner tumors of the ovary make ultrasonographic diagnosis more difficult. There are no special ultrasonographic features that can characterize benign brenner tumors. However, it is worth noting that some ultrasonographic features, including calcification with shadow, poor blood circulation of solid components, and tumor location, may be signs of benign brenner tumors and even help experienced ultrasonography doctors to preliminarily determine the benign and malignant nature of lesions. However, this study was a single-center study with a small sample size. In the future, a multi-center study with a larger sample size may draw a more convincing conclusion.

Acknowledgments

Not applicable.

Funding

This study was supported by a grant from the Medical Research Project of the Sichuan Medical Association (No. s19332).

Conflicts of interest

The authors indicated no potential conflicts of interest.

Author contributions

Not applicable.

Data availability statement

Not applicable.

Ethical approval

Not applicable.

References

1. Tamás J, Vereczkey I, Tóth E, et al. Mixed ovarian tumor composed of Brenner tumor and adult-type granulosa cell tumor: a case report of a very rare mixed ovarian tumor and a review of the literature. Int J Surg Pathol. 2018;26(4):382-387.
2. Lin DI, Killian JK, Venstrom JM, et al. Recurrent urothelial carcinoma-like FGFR3 genomic alterations in malignant Brenner tumors of the ovary. Mod Pathol. 2021;34(5):983-993.
3. Pfarr N, Darb-Esfahani S, Leichsenring J, et al. Mutational profiles of Brenner tumors show distinctive features uncoupling urothelial carcinomas and ovarian carcinoma with transitional cell histology. Genes Chromosomes Cancer. 2017;56(10):758-766.
4. Simons M, Simmer F, Bulten J, et al. Two types of primary mucinous ovarian tumors can be distinguished based on their origin. Mod Pathol. 2020;33(4):722-733.
5. López MM, González PL, Domingo ÁG, et al. Tumor de brenner benigno asociado a tumor mucinoso borderline de ovario en paciente postmenopáusica. Clínica e Investigación en Ginecología y Obstetricia. 2021;48(2):156-160.
6. Bazot M, Thomassin-Naggara, Daraï E. CT and MR imaging of ovarian adenocarcinoma (serous/mucinous/endometrioid). Ovarian Neoplasm Imaging. 2013.243-262.
7. Stukan M, Badocha M, Ratajczak K. Development and validation of a model that includes two ultrasound parameters and the plasma D-dimer level for predicting malignancy in adnexal masses: an observational study. BMC Cancer. 2019;19(1):564.
8. Dierickx I, Valentin L, Van Holsbeke C, et al. Imaging in gynecological disease (7): clinical and ultrasound features of Brenner tumors of the ovary. Ultrasound Obstet Gynecol. 2012;40(6):706-713.
9. Patel-Lippmann KK, Sadowski EA, Robbins JB, et al. Comparison of international ovarian tumor analysis simple rules to society of radiologists in ultrasound guidelines for detection of malignancy in adnexal cysts. AJR Am J Roentgenol. 2020;214(3):694-700.
10. Ordóñez NG, Mackay B. Brenner tumor of the ovary: a comparative immunohistochemical and ultrastructural study with transitional cell carcinoma of the bladder. Ultrastruct Pathol. 2000;24(3):157-167.
11. He B, Gong S, Hu C, et al. Obscure gastrointestinal bleeding: diagnostic performance of 64-section multiphase CT enterography and CT angiography compared with capsule endoscopy. Br J Radiol. 2014;87(1043):20140229.
12. Buscail L, Bournet B, Cordelier P. Role of oncogenic KRAS in the diagnosis, prognosis and treatment of pancreatic cancer. Nat Rev Gastroenterol Hepatol. 2020;17(3):153-168.

DOI 10.1007/s10330-021-0533-3
Cite this article as: Wang SY, Zhou XM. Ultrasonographic and clinicopathologic features of benign brenner tumors of the ovary. Oncol Transl Med. 2022;8(3):146–149.

Oncology and Translational Medicine
DOI 10.1007/s10330-021-0520-0

June 2022, Vol. 8, No. 3, P150–P153

CASE REPORT

Spindle epithelial tumor with thymus-like differentiation: A case report and literature review*

Li Zheng (✉), Jin Wang, Lin Ang, Jin Huang, Min Zhao (✉)

Department of Pathology, The Second People's Hospital of Hefei, Hefei 230011, China

Abstract

Spindle epithelial tumor with thymus-like differentiation (SETTLE) is a rare, low-grade malignant neoplasm that mainly occurs in the thyroid gland or its perimeter. Fewer than 10 cases of SETTLE have been reported in the Chinese literature, whereas approximately 50 cases have been reported in the international literature. We report a rare case of SETTLE that occurred in the soft tissues of the neck around the thyroid gland in a 41-year-old man. The neoplastic tissue, which mainly consisted of spindle epithelial components, included sporadically visible thymus-like structures. Immunohistochemistry demonstrated CK and CK19 positivity in the thymic epithelial components and CK, vimentin, and Bcl-2 positivity in the spindle cells. Surgical resection is the main treatment option for SETTLE. This patient underwent mass resection of the neck, and no recurrence or metastasis was observed even at 8 months postoperatively.

Received: 11 September 2021
Revised: 21 November 2021
Accepted: 15 January 2022

Key words: spindle epithelial tumor; thymus-like differentiation; immunohistochemistry

Spindle epithelial tumor with thymus-like differentiation (SETTLE) is a rare, low-grade thymic malignancy. Histologically, SETTLE presents with a lobulate structure and a biphasic cellular association characterized by spindle epithelial cells mixed with thymic structures. It primarily occurs in or around the thyroid gland. In this paper, we report a case of SETTLE, which developed in the soft tissues of the neck around the thyroid gland and discuss its clinicopathological features and differential diagnoses to improve the understanding of this tumor.

Materials and methods

A 41-year-old man presented with an incidentally discovered mass on the right side of the neck one week ago. He did not experience any obvious discomfort. Physical examination revealed that the mass, located on the right anterior side of the neck above the clavicle, was palpable and measured approximately 4.0 cm in diameter. No tenderness or restriction of neck movement was evident. Computed tomography revealed a soft tissue shadow in the right parathyroid gland. An ultrasound B-scan showed a deep-seated subcutaneous hypo echoic nodule in the neck, not occupying the thyroid gland. Results of serology tests showed that levels of thyroglobulin, thyroglobulin antibodies, thyroxine, and other thyroid function parameters were within the reference range. The right cervical mass was resected clinically.

The surgical specimen was fixed with 10% neutral-buffered formalin solution, paraffin-embedded, and routinely sectioned for histological analysis. Immunohistochemical analysis was performed using a Roche automatic immunohistochemistry staining machine. CK, EMA, CK19, vimentin, SMA, desmin, STAT-6, Bcl-2, S-100, TTF-1, TG, calcitonin, Syn, CD5, TdT, HMB45, and Ki-67 antibodies were commercially obtained from Fuzhou Maxim Biotechnology Co., Ltd. Each antibody was validated with positive and negative controls.

Results

Macroscopic examination revealed a piece of gray–red irregular tissue that was 6.0 cm × 3.0 cm × 1.5 cm in size

✉ Correspondence to: Min Zhao. Email: zhao.min.hi@163.com
Li Zheng. Email: zhengli352@163.com
* Supported by a grant from the Sixth Cycle Medical Key SpecialistConstruction Funds of Hefei (No. 2019(160)).

and characterized by a gray–white cut surface, tough texture, and intact envelope.

The neoplastic tissue was mainly composed of spindle-shaped cells (Fig. 1). The spindle-shaped cells were arranged in bundles and weaves with short spindle-shaped nuclei and fine chromatin. Nucleoli could not be discerned easily. Few nuclear fission images were evident. Scattered thymus-like structures, arranged in a cystic or cord-like pattern, were visible inside the tissue (Fig. 2). Immunohistochemical analysis of the neoplastic thymic epithelial components revealed positive staining for CK (Fig. 3) and CK19 and partially positive staining for CK7. Further, the tumor was positive for CK, Bcl-2, and vimentin (Fig. 4), partially positive for SMA, and negative for TTF-1, TG, calcitonin, CD5, TdT, CD5, CEA, HMB45, SATA-6, Syn, and desmin in spindle cells. The Ki-67 index was approximately 5%.

Discussion

SETTLE is believed to emanate from ectopic thymic tissue or the remnants of the branchial sac. It often develops in children, adolescents, and young adults with a mean age of onset of 19 (ranged, 4–59) years. However, SETTLE has also been reported in older adults, albeit rarely, and is more common in males. To the best of our knowledge, fewer than 10 cases have been reported in the Chinese literature, whereas approximately 50 cases have been reported in the international literature [1-5]. The youngest patient reported in the literature was a 2-year-old child [6, 7], whereas the oldest patient was a 75-year-old man [8]. A painlessly growing thyroid mass is the primary clinical sign. A rapidly enlarging mass in the neck, local tenderness, and tracheal compression are uncommon manifestations. Thyroid function is unaffected, and results of pathological investigations such as CEA and calcitonin levels do not show any abnormalities. No susceptibility factor (e.g., iodine deficiency, ionizing radiation, genetics, or environment) is associated with the development of SETTLE. It mainly occurs in the thyroid gland, but it can also occur in the soft tissues surrounding the thyroid gland. This case features a lesion occupying the soft tissues surrounding the thyroid gland.

SETTLE is a spindle epithelial neoplasm. The tumor is commonly bifurcated and characterized by spindle-shaped epithelial cells mixed with thymus-like structures. However, rarely, it can be unidirectional and consist of spindle cells or thymus-like structures

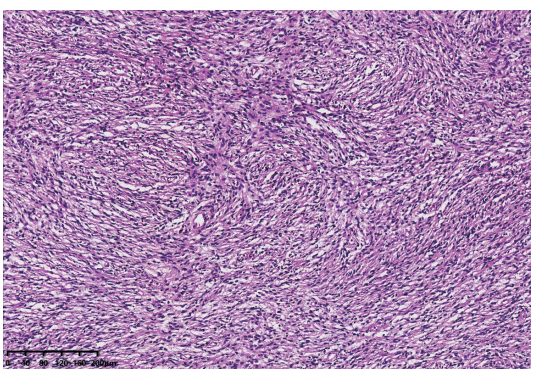

Fig. 1 The tumor predominantly spindle cells arranged in bundles or weaves (HE staining × 100)

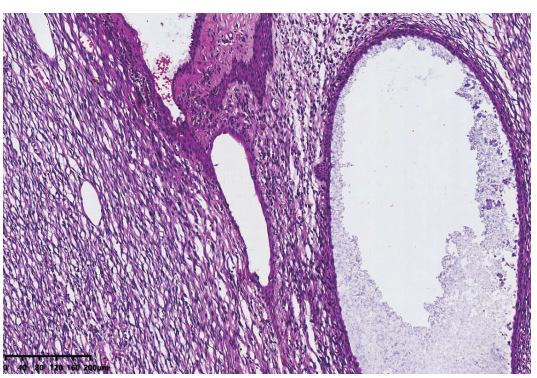

Fig. 2 Cystic thymic structures seen between the spindle cells (HE staining × 100)

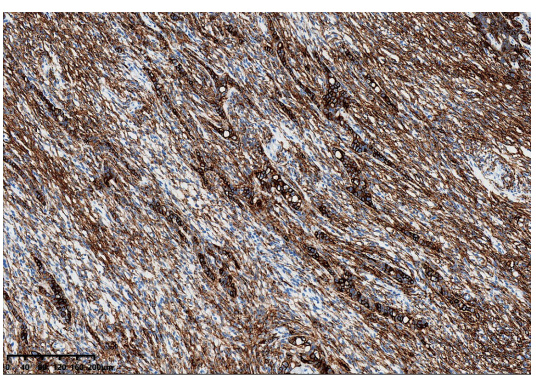

Fig. 3 CK positive in spindle cells and thymic epithelium, stained by automatic immunohistochemical staining machine (IHC × 100)

Fig. 4 Vimentin-positive spindle cells, stained by automatic immunohistochemical staining machine (IHC × 100)

only. Spindle cells are not distinctly anisotropic. Spindle cells are characterized by little cytoplasm, long nuclei, fine chromatin, inconspicuous nucleoli, and rare nuclear fission. Spindle cells sporadically exhibit hyper-disintegrative activity and focal necrosis. The thymus-like component may be tubular, papillary, or cord-like or comprise small islands of lightly stained cells or epithelium-lined cystic lumens, with cuboidal or columnar cells lining the thymic ducts. This component can also be mucinous or accompanied by cilia with some squamous metaplasia observed in a few cases. There is no obvious lymphocytic infiltration. Immunohistochemically, both neoplastic components of SETTLE have an epithelial phenotype, express broad-spectrum CK, and have spindle cells that are positive for vimentin. Spindle cells also express SMA, c-kit, and Bcl-2 but do not express TG, TTF-1, calcitonin, S-100, Syn, and CgA. The diagnosis of SETTLE relies primarily on histological features and immunohistochemical phenotypes, and accurate preoperative cytological diagnosis is difficult. Kijong Yi *et al.* [9] reviewed eight cases in the literature that were diagnosed using fine needle aspiration cytology. These cases were described only morphologically with respect to cytological diagnosis.

SETTLE should be differentiated from neoplasms with a spindle cell component.

Synovial sarcoma is a mesenchymal-derived spindle cell tumor with some degree of epithelial differentiation, including gland formation. It can affect any site, and approximately 5% of these tumors occur on the head and neck. Bidirectional synovial sarcoma has components of both epithelial and spindle cells, and the two components are present in variable proportions. The spindle-shaped tumor cells are distinctly anisotropic and relatively small and are characterized by oval nuclei; lightly stained, inconspicuous nucleoli; minimal cytoplasm; and poorly defined cells. The epithelial cells contain oval nuclei and abundant cytoplasm, forming thymus-like lumens containing epithelial mucus, which may also be papillary in structure. The interstitial collagen fibers are sparse and may become focally mucinous or focally calcified. The tumors may contain large numbers of mast cells. The tumors express cytokeratin CK, EMA, vimentin, CD99, BCL-2, and calponin, but not desmin or CD34. Furthermore, t(X; 18) (p11; q11) is a specific cytogenetic marker for this neoplasm and can be ascertained by molecular biology testing for cases in which differentiation of SETTLE seems difficult.

Ectopic malformed thymoma is a benign tumor arising from the superficial or deep soft tissues of the neck. It has both ectopic and neoplastic features and is most commonly observed in males. This tumor is similar in origin to SETTLE, and it is considered to be one of the tumors of the neck that is associated with parotid or gill bursal derivatives. The tumor consists of a mixture of spindle cells, islands of epithelial cells, and adipose tissue. The spindle cells were predominantly arranged in bundles but may also be of woven or matted shapes, containing fat spindle-shaped or elongated nuclei, fine chromatin or vacuole-like, small nucleoli, and non-isomorphic nuclei. Epithelial cells often appear as islands, small nests, or dilated cysts, and epithelial cells often show squamous epithelial differentiation, which may be accompanied by the formation of a varying number of thymic ducts. Immunohistochemistry revealed the myoepithelial differentiation of spindle cells, signifying that neoplasms or tumor cells are a mixture of epithelial cells and myoepithelial cells. Immunohistochemically, epithelial cells express epithelial markers, such as CK, CK5, CK6, CK7, CK8, and EMA, whereas spindle cells express epithelial markers, CD34, and CD10, with some of them expressing MSA, a-SMA, and calponin.

Carcinoma with thymus-like differentiation usually occurs in the lower end of the thyroid gland and, rarely, in the soft tissues surrounding the thyroid gland. Morphologically similar to thymic carcinoma, the tumor is characterized by squamous cell-like or syncytial cells and a pale eosinophilic cytoplasm. The tumor cells are short, and are spindle-shaped or polygonal, containing a poorly defined cell contour and a mild-to-moderate atypical, large, ovoid, or vesicular nucleus with a mitotic count of 1–2/10 HPF. Tumor cells may be associated with squamous differentiation, and lymphocytic infiltration of intercellular substances may be noted. Immunohistochemistry revealed the expression of CD5 and CD117 in addition to that of Bcl-2, Mcl-1, CK, EMA, and CEA. TTF-1 expression was absent.

Sarcomatous undifferentiated carcinoma is a highly malignant, extensively invasive tumor consisting of a mixture of spindle cells, pleomorphic giant cells, and epithelioid cells. When the tumor is predominantly composed of spindle cells, it often exhibits a sarcomatous form, featuring a fascicular or matted arrangement of cells as well as marked anisotropy and pleomorphism. Immunohistochemistry revealed strong positivity for CK and TP53 with minimal or no TG and TTF-1 expression.

Medullary thyroid carcinomas are a group of malignant neoplasms that emanate from parafollicular cells of the thyroid gland and exhibit varied histological patterns. Some medullary carcinomas may consist mainly of spindle-shaped cells arranged in bundles, which are known as spindle cell medullary carcinomas. Although this form is uncommon, it is important to differentiate it from SETTLE. Amyloid deposits are often noted in medullary carcinomas, and immunohistochemistry showed positivity for calcitonin and some neuroendocrine markers, such as CD56 and Syn.

Other tumors with a spindle cell component, such as

isolated fibrous tumors, malignant fibrous histiocytoma, and malignant melanoma, can be accurately identified using the knowledge of SETTLE histological patterns and assistance from differential immunohistochemical markers.

Although SETTLE is a low-grade malignancy, distant metastasis is possible, with the lung being the most common site of metastasis. In some cases, SETTLE lesions also metastasize to the lymph nodes, bones, and kidneys. Distant SETTLE metastases generally occur at a late stage, up to 25 years after the initial diagnosis [10]. Even in the presence of metastatic lesions, the patient can still survive for a long time after treatment. However, there have been some reports on short-term metastases and even patient death [11]. The treatment of SETTLE primarily involves surgical resection. Chemotherapy and radiotherapy may represent a feasible approach for patients with advanced disease to control tumor growth, local infiltration, and bloodstream metastasis. Since late metastases may occur, long-term follow-up is recommended to detect such cases [12]. In our patient, no tumor recurrence or metastasis was observed even at postoperative 8-month follow-up.

Acknowledgments

Not applicable.

Funding

This study was supported by a grant from the Sixth Cycle Medical Key SpecialistConstruction Funds of Hefei (No. 2019(160)).

Conflicts of interest

The authors indicated no potential conflicts of interest.

Author contributions

All authors contributed to data acquisition, data interpretation, and reviewed and approved the final version of this manuscript.

Data availability statement

The data that support the findings of this study are available from the corresponding author upon reasonable request.

Ethical approval

Not applicable.

References

1. Yue ZY, Guo SJ, Miao J, et al. Two reported cases of thymic spindle neoplasm with thymus-like differentiation. J Diag Pathol (Chinese). 2017;24(9):703-705.
2. Xie N, Huang YS, Xue FG, et al. Clinicopathological observation of thymus- or gill-bladder-associated tumors in the thyroid gland. Hainan Med J (Chinese). 2014;25(2):277-280.
3. Xu H, Yang CW, Yang SJ. Report of a case of papillary thyroid carcinoma with thymus-like differentiation of spindle cell tumor and lymph node metastasis in the thyroid gland. J Diag Pathol (Chinese). 2012;19(6):464-465.
4. Su HY, Wu WQ, Shen HW. Cloacal epithelial tumor of the thyroid gland with thymus-like differentiation. Chin J Pathol (Chinese). 2006;35(1):61.
5. Misra RK, Mitra S, Yadav R, et al. Spindle epithelial tumor with thymus-like differentiation: a case report and review of literature. Acta Cytol. 2013;57(3):303-308.
6. Casco F, Illanes Moreno M, González Cámpora R, et al. Spindle epithelial tumor with thymuslike differentiation in a 2-year-old boy: a case report. Anal Quant Cytol Histol. 2010;32(1):53-57.
7. Satoh S, Toda S, Narikawa K, et al. Spindle epithelial tumor with thymus-like differentiation (SETTLE): youngest reported patient. Pathol Int. 2006;56(9):563-567.
8. Zhang XW, Huang BF, Wu KB. Spindle epithelial tumor with thymus-like differentiation of the thyroid: a case report. Chin J Anat Clin. 2019;24(1):87-88.
9. Yi K, Rehman A, Jang SM, et al. Review of the touch preparation cytology of spindle epithelial tumor with thymus-like differentiation. J Cytol. 2016;33(1):27-29.
10. Karaisli S, Haciyanli M, Gücek Haciyanli S, et al. Spindle epithelial tumour with thymus-like differentiation: report of two cases. Ann R Coll Surg Engl. 2020;102(2):e33-e35.
11. Cheuk W, Jacobson AA, Chan JK. Spindle epithelial tumor with thymus-like differentiation (SETTLE): a distinctive malignant thyroid neoplasm with significant metastatic potential. Mod Pathol. 2000;13(10):1150-1155.
12. Ippolito S, Bellevicine C, Arpaia D, et al. Spindle epithelial tumor with thymus-like differentiation (SETTLE): clinical-pathological features, differential pathological diagnosis and therapy. Endocrine. 2016;51(3):402-412.

DOI 10.1007/s10330-021-0520-0
Cite this article as: Zheng L, Wang J, Ang L, et al. Spindle epithelial tumor with thymus-like differentiation: A case report and literature review. Oncol Transl Med. 2022;8(3):150–153.

Call For Papers
Oncology and Translational Medicine

(CN 42-1865/R, ISSN 2095-9621)

Dear Authors,

Oncology and Translational Medicine (OTM), a peer-reviewed open-access journal, is very interested in your study. If you have unpublished papers in hand and have the idea of making our journal a vehicle for your research interests, please feel free to submit your manuscripts to us via the Paper Submission System.

Aims & Scope

- Lung Cancer
- Liver Cancer
- Pancreatic Cancer
- Gastrointestinal Tumors
- Breast Cancer
- Thyroid Cancer
- Bone Tumors
- Genitourinary Tumors
- Brain Tumor
- Blood Diseases
- Gynecologic Oncology
- ENT Tumors
- Skin Cancer
- Cancer Translational Medicine
- Cancer Imageology
- Cancer Chemotherapy
- Radiotherapy
- Tumors Psychology
- Other Tumor-related Contents

Contact Us
Editorial office of Oncology and Translational Medicine
Tongji Hospital
Tongji Medical College
Huazhong University of Science and Technology
Jie Fang Da Dao 1095
430030 Wuhan, China
Tel.: 86-27-69378388
Email: dmedizin@tjh.tjmu.edu.cn;
dmedizin@sina.com

Oncology and Translational Medicine (OTM) is sponsored by Tongji Hospital, Tongji Medical College, Huazhong University of Science and Technology, China (English, bimonthly).

OTM mainly publishes original and review articles on oncology and translational medicine. We are working with the commitment to bring the highest quality research to the widest possible audience and share the research work in a timely fashion.

Manuscripts considered for publication include regular scientific papers, original research, brief reports and case reports. Review articles, commentaries and letters are welcome.

About Us

- Peer-reviewed
- Rapid publication
- Online first
- Open access
- Both print and online versions

For more information about us, please visit:
http://otm.tjh.com.cn